NASA TECHNICAL NOTE

NASA TN D-5038

C. 1

NASA TN D-5038

THE ADMITTANCE OF A PARALLEL-PLATE APERTURE ILLUMINATING A DISPLACED DIELECTRIC-DIELECTRIC BOUNDARY

by J. Earl Jones

Langley Research Center
Langley Station, Hampton, Va.

NATIONAL AERONAUTICS AND SPACE ADMINISTRATION • WASHINGTON D. C. • FEBRUARY 1969

NASA TN D-5038

THE ADMITTANCE OF A PARALLEL-PLATE APERTURE ILLUMINATING A DISPLACED DIELECTRIC-DIELECTRIC BOUNDARY

By J. Earl Jones

Langley Research Center
Langley Station, Hampton, Va.

NATIONAL AERONAUTICS AND SPACE ADMINISTRATION

For sale by the Clearinghouse for Federal Scientific and Technical Information
Springfield, Virginia 22151 – CFSTI price $3.00

THE ADMITTANCE OF A PARALLEL-PLATE APERTURE ILLUMINATING A DISPLACED DIELECTRIC-DIELECTRIC BOUNDARY

By J. Earl Jones
Langley Research Center

SUMMARY

The variational method is used to determine the admittance of a transverse-electromagnetic-mode excited, parallel-plate aperture having an infinite flange and illuminating a displaced dielectric-dielectric boundary. The results are applied to provide insight into two problems of interest: (a) the effect of an air gap on the admittance of dielectric-coated aperture antennas and (b) the admittance of an aperture antenna coated with an underdense plasma slab. Numerical computations for the air-gap problem are verified experimentally.

For either problem, the most significant changes in the admittance occur for displacements less than 0.25 wavelength. (The wavelength referred to is the free-space wavelength divided by the square root of the relative permittivity of the medium between the boundary and the aperture.) For the dielectric-coated slot antenna, changes in the admittance due to an air gap are enhanced if either the slot width is reduced or the permittivity is increased. For a slot antenna coated with a thin underdense plasma slab, the admittance becomes more sensitive to changes in the layer thickness as the plasma becomes more dense. As observed theoretically for both the air-gap problem and the underdense-plasma problem, the admittance is not influenced by the presence of surface waves. Experimental verification of this result is given for the air-gap problem.

INTRODUCTION

Flush-mounted aperture antennas covered by low-loss dielectrics are frequently used as radomes or for thermal protection of spacecraft antennas on reentry vehicles. Air gaps between the aperture surface and the dielectric often result from construction errors and unequal thermal expansion of the dielectric and metal surfaces. Such gaps cause appreciable changes in the admittance from design values. Other than experimental or empirical data, little quantitative information on such effects is presently available.

One useful model for gaining insight into the effects of an air gap on the admittance of a dielectric-coated aperture antenna is the ground-plane-mounted aperture illuminating

a dielectric layer of finite thickness and displaced a distance d. A two-dimensional version of this model has been treated by Burnside (ref. 1) using the wedge-diffraction method from reference 2 for the parallel-plate aperture. Although both finite and infinite layers were treated by this method, the results are not applicable for displacements less than 0.5 wavelength whenever the slot width is less than 1 wavelength (ref. 1) and, hence, are not applicable for air gaps of most sizes which occur in practice.

An alternate approach for obtaining results which are valid for displacements less than 0.5 wavelength is the variational method used in conjunction with Fourier transform theory (refs. 3 to 8). To achieve some basic insight into the effect of air gaps, the layer thickness will be assumed to be infinite in this paper. However, if in the theoretical derivation both the air layer and the infinite dielectric medium are assumed to be homogeneous dielectrics, the results can also be used to determine the admittance of a lossless, underdense plasma-coated aperture radiating into free space; the overdense plasma-coated aperture has been studied previously by Fante (ref. 9).

For both the air-gap problem and the underdense-plasma problem, numerical computations which show the influence of the permittivity, the slot width, and the layer thickness on the admittance are given. For the air-gap problem, the results are compared with the admittance of the same aperture radiating into a half-space having the same permittivity as that of the dielectric and also radiating into free space. Similarly, for the underdense-plasma problem, the results are compared with the admittance of the same aperture radiating into a half-space having the same permittivity as the plasma and also radiating into free space. Experimental verification of the theory for the air-gap problem is also given.

SYMBOLS

$A = 2\pi a_\lambda$

a	aperture width
a_λ	aperture width, free-space wavelengths
B	aperture susceptance
b	normalized aperture susceptance
$C_1^{(i)}(k_x), C_2^{(i)}(k_x)$	spectral constants
$C(\beta)$	normalized function

$D = 2\pi d_\lambda$

$D_A(\beta), D_B(\beta)$ normalized functions

d thickness of medium 1

d_λ thickness of medium 1, free-space wavelengths

$d_{\lambda e} = \sqrt{\mu_{r,1}\epsilon_{r,1}}\, d_\lambda$

E electric field intensity

$\overline{E}$ Fourier transform of electric field intensity

$F(x)$ function of x

$f(\beta)$ normalized function

f frequency

G aperture conductance

g normalized aperture conductance

H magnetic field intensity

$\overline{H}$ Fourier transform of magnetic field intensity

$H_0^{(2)}(x)$ Hankel function of the second kind of order zero and argument x

I reaction integral

I_1, I_2, I_3, I_4, I_5 integrals

$\mathrm{Im}(\ )$ imaginary part of complex variable

i medium, 1 or 2 (see fig. 1)

$J_x^{(1)}(x,0)$ surface electric current density on ground plane

$j = \sqrt{-1}$

k_i	propagation constant in medium i
k_x	x-directed propagation constant
$k_{z,i}$	z-directed propagation constant in medium i
k_0	free-space propagation constant
N_i	refractive index in medium i
n	variable of summation
R	reflection coefficient (current)
Re( )	real part of complex variable
$S_i(\beta)$	normalized function for medium i
t	time
$U(k_x)$	spectral function
V_o	aperture voltage
v	complex variable
x	dummy variable
x_λ	variable of integration
x,y,z	distance along X-, Y-, and Z-axis, respectively
Y	aperture admittance
$\overline{Y}$	Fourier transform of Y
Y_0	free-space characteristic admittance

y normalized aperture admittance

β normalized variable of integration

γ_n propagation constant

$\delta_0{}^n$ Kronecker delta; 1 when $n \neq 0$, 0 when $n = 0$

ϵ_i permittivity of medium i

$\epsilon_i' = \mathrm{Re}(\epsilon_i)$

$\epsilon_i'' = \mathrm{Im}(\epsilon_i)$

ϵ_r relative permittivity

$\epsilon_{r,i}$ relative permittivity of medium i

$\epsilon_{r,i}' = \mathrm{Re}(\epsilon_{r,i})$

$\epsilon_{r,i}'' = \mathrm{Im}(\epsilon_{r,i})$

ϵ_0 free-space permittivity

$\theta_i = \sqrt{\beta^2 - N_i{}^2}$

λ_0 free-space wavelength

μ_i permeability of medium i

$\mu_{r,i}$ relative permeability of medium i

μ_0 free-space permeability

$\phi_i = \sqrt{N_i{}^2 - \beta^2}$

ω angular frequency, radians per second

ω_p plasma frequency, radians per second

Subscripts:

i	medium, 1 or 2
x,y,z	component in x-, y-, and z-direction, respectively

Superscripts:

i	medium, 1 or 2
w	waveguide

Abbreviations:

SWR	standing-wave ratio
TE	transverse electric
TEM	transverse electromagnetic
TM	transverse magnetic

SYNOPSIS OF THEORY

The geometry of the problem under consideration is shown in figure 1. A synopsis of the theory necessary for determining the admittance of the aperture is given in this section; mathematical details are given in appendix A. The admittance is determined from the stationary expression

$$Y = G + jB = \frac{1}{|V_0|^2} \int_{-a/2}^{a/2} E_x^{(w)}(x,0)\, H_y^{(w)}(x,0)\, dx \tag{1}$$

where the aperture electric field $E_x^{(w)}(x,0)$ just inside the waveguide is given by $V_0/\sqrt{a}$ and where the time dependence $e^{j\omega t}$ for the fields is implicit. The boundary-value problem for the fields in the external medium is solved with the aid of Fourier transform theory. Application of the convolution theorem and the appropriate boundary conditions in the aperture plane leads to the result

$$Y = \frac{4}{\pi a}\int_0^\infty \frac{\sin^2\frac{k_x a}{2}}{k_x^2}\left[\frac{\omega\epsilon_1}{k_{z,1}}\left(\frac{1 + j\,\frac{k_{z,2}\epsilon_1}{k_{z,1}\epsilon_2}\tan k_{z,1}d}{\frac{k_{z,2}\epsilon_1}{k_{z,1}\epsilon_2} + j\tan k_{z,1}d}\right)\right]dk_x \tag{2}$$

where

$$k_{z,i} = \left(k_i^2 - k_x^2\right)^{1/2} \qquad \left(\mathrm{Re}\left(k_{z,i}\right) > 0;\quad \mathrm{Im}\left(k_{z,i}\right) \leqq 0\right)$$

and

$$k_i^2 = \omega^2\mu_i\epsilon_i$$

In appendix B this result is checked for several limiting cases of interest.

The integral in equation (2) is a contour integral along the entire positive k_x-axis in the v-plane, where $k_x = \mathrm{Re}(v)$. Consequently, in evaluating the integral it is necessary to include the residue contributions of the real axis poles which physically represent the propagation constants of TM (to the X-axis) surface wave modes in the layer. However, if the dielectric-dielectric boundary is a "rare-to-dense" type of boundary, that is, if $\epsilon_2' > \epsilon_1'$ for $\mu_2 = \mu_1 = \mu_0$ and $\epsilon_1'' = \epsilon_2'' = 0$, no surface wave poles occur and thus no energy is coupled into surface waves. Under this condition the integral in equation (2) can be easily evaluated by straightforward numerical integration. Also, to facilitate numerical computations, the admittance, the constitutive parameters, and the dimensions can be normalized to those of free space by letting $k_x = k_0\beta$. This normalization has been done in appendix C, and the final result is

$$y = \frac{Y}{Y_0} = \frac{G + jB}{Y_0} = g + jb \tag{3}$$

where

$$g = \frac{2\epsilon_{r,1}'}{\pi^2 a_\lambda}\left(I_1 + I_2\right) \tag{4}$$

$$b = \frac{2\epsilon_{r,1}'}{\pi^2 a_\lambda}\left(I_3 + I_4 + I_5\right) \tag{5}$$

$$I_1 = \epsilon_{r,1}'\epsilon_{r,2}'\int_0^{N_1}\frac{\phi_2}{D_A(\beta)}\,f(\beta)\,d\beta \tag{6}$$

$$I_2 = \epsilon_{r,1}'\epsilon_{r,2}'\int_{N_1}^{N_2}\frac{\phi_2}{D_B(\beta)}\,f(\beta)\,d\beta \tag{7}$$

$$I_3 = \int_0^{N_1} \frac{D\left(\epsilon'_{r,1}\phi_2\right)^2 \cos D\phi_1 \dfrac{\sin D\phi_1}{D\phi_1} - \left(\epsilon'_{r,2}\right)^2 \dfrac{\phi_1}{2} \sin 2D\phi_1}{D_A(\beta)} f(\beta)\, d\beta \tag{8}$$

$$I_4 = \int_{N_1}^{N_2} \frac{D\left(\epsilon'_{r,1}\phi_2\right)^2 \cosh D\theta_1 \dfrac{\sinh D\theta_1}{D\theta_1} + \left(\epsilon'_{r,2}\right)^2 \dfrac{\theta_1}{2} \sinh 2D\theta_1}{D_B(\beta)} f(\beta)\, d\beta \tag{9}$$

$$I_5 = \int_{N_2}^{\infty} \frac{\epsilon'_{r,2} + \dfrac{\theta_2}{\theta_1}\epsilon'_{r,1} \tanh D\theta_1}{\epsilon'_{r,1}\theta_2 + \epsilon'_{r,2}\theta_1 \tanh D\theta_1} f(\beta)\, d\beta \tag{10}$$

$$D_A(\beta) = \left(\epsilon'_{r,1}\phi_2\right)^2 \cos^2 D\phi_1 + \left(\epsilon'_{r,2}\phi_1\right)^2 \sin^2 D\phi_1 \tag{11}$$

$$D_B(\beta) = \left(\epsilon'_{r,1}\phi_2\right)^2 \cosh^2 D\theta_1 + \left(\epsilon'_{r,2}\theta_1\right)^2 \sinh^2 D\theta_1 \tag{12}$$

and where

$$f(\beta) = \frac{\sin^2 \pi\lambda\beta}{\beta^2}$$

$$\phi_i = \sqrt{N_i^2 - \beta^2}$$

$$\theta_i = \sqrt{\beta^2 - N_i^2}$$

$$N_i = \sqrt{\mu_{r,i}\epsilon'_{r,i}}$$

$$D = 2\pi d_\lambda$$

$$d_\lambda = d/\lambda_0$$

$$a_\lambda = a/\lambda_0$$

$$\mu_{r,i} = \mu_i/\mu_0$$

and

$$\epsilon'_{r,i} = \epsilon'_i / \epsilon_0$$

The reflection coefficient (current) is found from the relation

$$R = \frac{y - 1}{y + 1}$$

NUMERICAL COMPUTATIONS AND EXPERIMENT

The normalized equations given in the preceding section were programed on a digital computer and computations of y and R were obtained for the parameters given in the following table:

Problem	Fixed parameters	Variable parameters	Experimental
Air gap	$\mu_{r,1} = \mu_{r,2} = 1$ $\epsilon'_{r,1} = 1$ $\epsilon''_{r,1} = \epsilon''_{r,2} = 0$	$a_\lambda = 0.03$ to 0.6 $\epsilon'_{r,2} = 2.05$ to 9 $d_\lambda = 0$ to 2.5	$a_\lambda = 0.332$ $\epsilon'_{r,2} = 2.55, 2.57$ $d_\lambda = 0$ to 1.0
Underdense plasma	$\mu_{r,1} = \mu_{r,2} = 1$ $\epsilon'_{r,2} = 1$ $\epsilon''_{r,1} = \epsilon''_{r,2} = 0$	$a_\lambda = 0.03$ to 0.6 $\epsilon'_{r,i} = 0.05$ to 0.8 $d_{\lambda e} = 0$ to 1.0	None

Experimental verification of the theory for the air-gap problem was obtained with the apparatus shown in figure 2. The infinitely thick coating in the theoretical model was simulated by a dielectric slab in the experimental model. Two sets of data were obtained, one with a plexiglass slab having a thickness of 0.983 in. (2.497 cm) and a relative permittivity of 2.57 and one with a polystyrene slab having a thickness of 2.010 in. (5.105 cm) and a relative permittivity of 2.55. The plexiglass slab was 4.75 wavelengths thick and the polystyrene slab was 9.71 wavelengths thick, with respect to the constitutive parameters of the dielectric at 35.7 GHz, the operating frequency. For either set of data, as indicated in figure 3, excellent agreement is obtained in the near field (that is, for $d_\lambda < 0.5$) of the aperture, although the theoretical results include only the dominant mode as the trial field. Similar observations regarding the usefulness of the dominant-mode assumption in determining the admittance of aperture antennas have also been made for both the rectangular (ref. 5) and circular (ref. 6) apertures in the presence of dielectrics. The minor disagreement between theory and experiment for $d_\lambda > 0.5$ is believed to be caused by the presence of the back wall of the slab in the experimental model (ref. 1).

Numerical computations of y for the same aperture radiating into a homogeneous half-space (ref. 3) for various relative permittivities as a function of a_λ (denoted by tick marks) are shown in figure 4 and serve as a useful check case for the limiting values of $d_{\lambda e}$. For $d_{\lambda e} = 0$ (that is, in the absence of an air gap or an underdense plasma), the value of y for the air-gap problem is on the locus corresponding to the relative permittivity of the coating and at the given value of a_λ and the value of y for the underdense-plasma problem is on the free-space locus and at the given value of a_λ. Similarly, for $d_{\lambda e} = \infty$ (that is, an infinitely thick air gap or underdense plasma), the value of y for the air-gap problem is on the free-space locus and the value of y for the underdense-plasma problem is on the locus corresponding to the relative permittivity of the plasma.

Numerical computations are given in figures 5 and 6 for the range of parameters listed in the table. Figure 5 shows the effect of the air-gap thickness d_λ upon the admittance for various aperture sizes and dielectric constants. The values chosen for the dielectric constants in figures 5(a), 5(b), and 5(c), respectively, correspond approximately to those of polytetrafluoroethylene (teflon), fused quartz, and alumina.

In figure 6, the admittance with an underdense plasma slab is plotted as a function of the plasma thickness for various combinations of plasma densities and aperture sizes. The values chosen for the relative permittivities in figures 6(a), 6(b), and 6(c), respectively, correspond to plasma electron densities of 0.5, 0.8, and 0.95 times critical density.

DISCUSSION

It is evident from the admittance loci in both figures 5 and 6 that the most significant changes in y occur whenever the displaced boundary lies in the near field of the aperture; more specifically, for $d_{\lambda e} < 0.25$. It is also evident that this result is independent of a_λ and $\epsilon'_{r,2}$ for the air-gap problem (fig. 5) or of a_λ and $\epsilon'_{r,i}$ for the underdense-plasma problem (fig. 6). For $d_{\lambda e} > 0.25$, the locus, and hence $|R|$, merely oscillates about the value of y obtained from figure 4 for $\epsilon_r = \epsilon'_{r,1}$.

For the air-gap problem the amplitude of the $|R|$ oscillations increases with an increase in either the slot width or the permittivity, or both. This observation can be deduced physically: an increase in a_λ increases both the directivity and the effective aperture so that more energy is collected when reflected from the boundary; also, an increase in $\epsilon'_{r,2}$ causes more energy to be reflected at the boundary. The air-gap tolerance effect (that is, the sensitivity of y with respect to d_λ in the near field) is also enhanced for increased values of the relative permittivity but is primarily dependent on the slot width, becoming extremely sensitive for narrow slots. As a numerical

example, for a narrow slot $(a_\lambda = 0.1)$ at a frequency of 35.7 GHz and a hard dielectric boundary $(\epsilon'_{r,2} = 9)$, $|R|$ is decreased from 0.56 to 0.24 for an air gap of only 0.008 in. (0.02032 cm).

For the underdense-plasma problem, as for the air-gap problem, the oscillations in $|R|$ as a function of the layer thickness are increased with an increase in the slot width for any given value of relative permittivity. Moreover, for a given aperture the sensitivity of y becomes more enhanced as the plasma becomes more dense; that is, as ω_p approaches ω or as $\epsilon'_{r,1}$ approaches zero.

The admittance locus for $a_\lambda = 0.6$ and $\epsilon'_{r,1} = 0.05$ in figure 6 is an interesting indication of how a thin plasma slab, close to critical density $(\omega_p/\omega = 0.975)$, will severely mismatch a spacecraft antenna previously matched to free space $(d_{\lambda e} = 0)$. For example, $|R|$ is increased from 0.11 to 0.66 for a layer only 1/20 wavelength thick, with respect to the plasma parameters.

An observation of practical interest concerns the absence of surface wave effects in equation (2) for the air-gap problem and the significance of the experimental data in figure 3. In a similar problem where medium 2 is a perfect conductor (ref. 8), it was noted that the value of y was determined by surface waves. Where medium 2 is a perfect conductor, the surface wave modes set up in medium 1 are actually waveguide modes. When experimental verification of the theory was sought by use of finite metal plates to simulate the infinite plates in the theoretical model, large scatter occurred in the data of $|R|$ as a function of d_λ. The scatter was due to the onset of propagation and the resulting mismatch of the modes at the terminations of the metal plates (see ref. 8 for a more complete discussion) and was evident to some extent even when the edges were curled to improve the match. (See figs. 5 and 8 of ref. 8.) It is evident in figure 3, however, that no appreciable scatter occurred, although the edges at the terminations were much more abrupt than in the metal-sheet problem. These observations further reveal that scatter in the experimental data for $|R|$ as a function of d_λ, when finite surfaces are used to simulate infinite surfaces, is caused by the mismatch of surface wave modes at the terminations.

CONCLUDING REMARKS

A variational method has been used to determine the admittance of a transverse-electromagnetic-mode excited, parallel-plate aperture having an infinite flange and illuminating a displaced dielectric-dielectric boundary. The results were used to provide insight into two problems of interest: (a) the effect of an air gap on the admittance of dielectric-coated aperture antennas and (b) the admittance of an aperture antenna coated with an underdense plasma slab. Numerical computations for the air-gap problem were verified experimentally.

The most significant changes in the admittance were found to occur for displacements less than 0.25 wavelength. (The wavelength referred to is the free-space wavelength divided by the square root of the relative permittivity of the medium between the boundary and the aperture.) For the dielectric-coated slot antenna, perturbations in the admittance due to an air gap were found to be enhanced if either the slot width is reduced or the permittivity is increased. For a slot antenna coated with a thin underdense plasma slab, the admittance was found to become more sensitive with respect to the layer thickness as the plasma becomes more dense.

It was deduced theoretically for both the air-gap problem and the underdense-plasma problem that the admittance is not influenced by the presence of surface waves. This deduction was verified experimentally for the air-gap problem.

Langley Research Center,
National Aeronautics and Space Administration,
Langley Station, Hampton, Va., November 19, 1968,
125-22-02-02-23.

APPENDIX A

DERIVATION OF THE ADMITTANCE EXPRESSION

The purpose of this appendix is to present the mathematical details leading to the development of equation (2). The general geometry of the problem, shown in figure 1, consists of a TEM mode excited, parallel-plate aperture having an infinite flange and radiating into a half-space environment consisting of (1) a lossy homogeneous dielectric layer of thickness d and with constitutive parameters μ_1 and $\epsilon_1 = \epsilon_1' - j\epsilon_1''$ and (2) a lossy homogeneous infinite medium with constitutive parameters μ_2 and $\epsilon_2 = \epsilon_2' - j\epsilon_2''$. The time convention $e^{j\omega t}$ for the fields is used throughout the deviation.

An expression for the admittance of a dominant-mode excited, ground-plane-mounted, cylindrical waveguide of arbitrary cross section is derived in reference 3 (pp. 8-12) in terms of the aperture electric and magnetic fields just inside the waveguide. It is further shown (ref. 3, pp. 12-16) that this expression is stationary with respect to small variations in the true value of the aperture electric field, provided the fields in the environment into which the aperture radiates satisfy the radiation conditions. For the aperture in figure 1, this expression reduces to

$$Y = \frac{I}{V_o^2} \tag{A1}$$

where I, the reaction integral, is

$$I = \int_{-a/2}^{a/2} E_x^{(w)}(x,0)\, H_y^{(w)}(x,0)\, dx \tag{A2}$$

and where the aperture field is assumed to consist of the incident and the reflected TEM mode; that is

$$\left.\begin{aligned} E_x^{(w)}(x,0) &= \frac{V_o}{\sqrt{a}} \qquad \left(|x| \leq \frac{a}{2}\right) \\ E_x^{(w)}(x,0) &= 0 \qquad \left(|x| > \frac{a}{2}\right) \end{aligned}\right\} \tag{A3}$$

The normalizing factor $\frac{1}{\sqrt{a}}$ in equation (A3) is necessary in order that the orthonormal property for the TEM mode function be satisfied. (See, for example, ref. 10.)

The reaction integral in equation (A2) can be evaluated by considering the assumed aperture electric field to be an equivalent magnetic surface current source for the fields in the external environment ($z > 0$) and solving for the magnetic field arising in the aperture as a result. For the two-dimensional problem under consideration, it is well known

that the Maxwell equations can be decoupled into two independent sets, one TE and one TM to the Y axis. Thus, with TEM mode excitation, the fields in both mediums 1 and 2 must satisfy the TM-decoupled wave equation

$$\frac{\partial^2 H_y^{(i)}(x,z)}{\partial x^2} + \frac{\partial^2 H_y^{(i)}(x,z)}{\partial z^2} + k_i^2 H_y^{(i)}(x,z) = 0 \tag{A4}$$

and the TM-decoupled Maxwell equation

$$E_x^{(i)}(x,z) = -\frac{1}{j\omega\epsilon_i} \frac{\partial H_y^{(i)}(x,z)}{\partial z} \tag{A5}$$

where

$$k_i = \omega^2 \mu_i \epsilon_i \tag{A6}$$

and $i = 1$ or 2.

Equations (A4) and (A5) must also satisfy the following boundary conditions:

$$E_x^{(1)}(x,d) = E_x^{(2)}(x,d) \tag{A7}$$

$$H_y^{(1)}(x,d) = H_y^{(2)}(x,d) \tag{A8}$$

$$E_x^{(1)}(x,0) = E_x^{(w)}(x,0) = \frac{V_o}{\sqrt{a}} \qquad \left(|x| \leq \frac{a}{2}\right) \tag{A9a}$$

$$E_x^{(1)}(x,0) = 0 \qquad \left(|x| > \frac{a}{2}\right) \tag{A9b}$$

$$H_y^{(1)}(x,0) = H_y^{(w)}(x,0) \qquad \left(|x| \leq \frac{a}{2}\right) \tag{A10a}$$

$$H_y^{(1)}(x,0) = -J_x^{(1)}(x,0) \qquad \left(|x| > \frac{a}{2}\right) \tag{A10b}$$

as well as the boundary condition requiring only outgoing waves at infinity. All these boundary conditions are readily enforceable except equation (A10b), since the ground-plane surface current arising as a result of the source field in the aperture cannot readily be determined. An alternate boundary condition is achieved by requiring the conservation of reaction (ref. 11, pp. 420-421) across the aperture. Thus

$$I = \int_{-a/2}^{a/2} E_x^{(w)}(x,0)\, H_y^{(w)}(x,0)\, dx = \int_{-a/2}^{a/2} E_x^{(1)}(x,0)\, H_y^{(1)}(x,0)\, dx \tag{A11}$$

The boundary-value problem for the fields in the external medium is easily solved by assuming Fourier transform solutions of the form

$$H_y^{(i)}(x,z) = \frac{1}{2\pi}\int_{-\infty}^{\infty} \overline{H}_y^{(i)}(k_x,z)e^{-jk_x x}\,dk_x \tag{A12}$$

thus reducing the number of independent variables in the wave equation from two to one, yielding the total differential equation

$$\frac{d^2\overline{H}_y^{(i)}(k_x,z)}{dz^2} + k_{z,i}^2\,\overline{H}_y^{(i)}(k_x,z) = 0 \tag{A13}$$

where

$$k_{z,i}^2 = k_i^2 - k_x^2 \tag{A14}$$

Similarly, substitution of equation (A12) into equation (A5) gives the transformed field equation

$$\overline{E}_x^{(i)}(k_x,z) = -\frac{1}{j\omega\epsilon_i}\frac{d\overline{H}_y^{(i)}(k_x,z)}{dz} \tag{A15}$$

and substitution of equation (A12) into equations (A7), (A8), and (A9) yields the transformed boundary conditions

$$\overline{E}_x^{(1)}(k_x,d) = \overline{E}_x^{(2)}(k_x,d) \tag{A16}$$

$$\overline{H}_y^{(1)}(k_x,d) = \overline{H}_y^{(2)}(k_x,d) \tag{A17}$$

$$\overline{E}_x^{(1)}(k_x,0) = \overline{E}_x^{(w)}(k_x,0) \tag{A18}$$

The general solution of equation (A13) is

$$\overline{H}_y^{(i)}(k_x,z) = C_1^{(i)}(k_x)e^{jk_{z,i}z} + C_2^{(i)}(k_x)e^{-jk_{z,i}z} \tag{A19}$$

which yields, when substituted into equation (A15), the result

$$\overline{E}_x^{(i)}(k_x,z) = -\frac{k_{z,i}}{\omega\epsilon_i}C_1^{(i)}(k_x)e^{jk_{z,i}z} + \frac{k_{z,i}}{\omega\epsilon_i}C_2^{(i)}(k_x)e^{-jk_{z,i}z} \tag{A20}$$

where the branch

$$k_{z,i} = \left(k_i^2 - k_x^2\right)^{1/2} \qquad \left(\mathrm{Re}(k_{z,i}) > 0;\quad \mathrm{Im}(k_{z,i}) \leq 0\right) \tag{A21}$$

must be chosen to satisfy the radiation condition for large values of z.

The spectral constants $C_1^{(1)}(k_x)$, $C_2^{(1)}(k_x)$, $C_1^{(2)}(k_x)$, and $C_2^{(2)}(k_x)$ are evaluated by applying equations (A16), A(17), and (A18) and requiring only outgoing waves for large z. This latter condition requires that $C_1^{(2)}(k_x) = 0$. Using this result and applying equations (A16) and (A17) to equations (A20) and (A19), respectively, give

$$-C_1^{(1)}(k_x)e^{jk_{z,1}d} + C_2^{(1)}(k_x)e^{-jk_{z,1}d} = \frac{\epsilon_1 k_{z,2}}{\epsilon_2 k_{z,1}} C_2^{(2)}(k_x)e^{-jk_{z,2}d} \tag{A22}$$

$$C_1^{(1)}(k_x)e^{jk_{z,1}d} + C_2^{(1)}(k_x)e^{-jk_{z,1}d} = C_2^{(2)}(k_x)e^{-jk_{z,2}d} \tag{A23}$$

Eliminating $C_2^{(2)}(k_x)$ from equations (A22) and (A23) gives

$$C_2^{(1)}(k_x) = U(k_x)C_1^{(1)}(k_x) \tag{A24}$$

where

$$U(k_x) = \frac{1 + \dfrac{k_{z,2}\epsilon_1}{k_{z,1}\epsilon_2}}{1 - \dfrac{k_{z,2}\epsilon_1}{k_{z,1}\epsilon_2}} e^{j2k_{z,1}d} \tag{A25}$$

Substitution of equation (A24) into equations (A19) and (A20) yields

$$\overline{H}_y^{(1)}(k_x,z) = \left[e^{jk_{z,1}z} + U(k_x)e^{-jk_{z,1}z}\right]C_1^{(1)}(k_x) \tag{A26}$$

and

$$\overline{E}_x^{(1)}(k_x,z) = -\frac{k_{z,1}}{\omega\epsilon_1}\left[e^{jk_{z,1}z} - U(k_x)e^{-jk_{z,1}z}\right]C_1^{(1)}(k_x) \tag{A27}$$

From the definition

$$\overline{Y}(k_x,z) = \frac{\overline{H}_y^{(1)}(k_x,z)}{\overline{E}_x^{(1)}(k_x,z)} \tag{A28}$$

it is evident that

$$\overline{Y}(k_x,z) = -\frac{\omega\epsilon_1}{k_{z,1}} \frac{e^{jk_{z,1}z} + U(k_x)e^{-jk_{z,1}z}}{e^{jk_{z,1}z} - U(k_x)e^{-jk_{z,1}z}} \tag{A29}$$

The solution is completed by applying the boundary conditions given in equations (A9) and (A11) in the Fourier transform domain. From equation (A9b) the limits of integration on the right side of equation (A11) can be extended to infinity without affecting the result. Furthermore, because of symmetrical excitation of the aperture, the fields everywhere are even functions of x. Then, by the convolution theorem

$$I = \int_{-\infty}^{\infty} E_x^{(1)}(x,0)\,H_y^{(1)}(x,0)\,dx = \frac{1}{2\pi}\int_{-\infty}^{\infty} \overline{E}_x^{(1)}(k_x,0)\,\overline{H}_y^{(1)}(k_x,0)\,dk_x \tag{A30}$$

Substituting equation (A28) into equation (A30) gives

$$I = \frac{1}{2\pi}\int_{-\infty}^{\infty} \overline{Y}(k_x,0)\left[\overline{E}_x^{(1)}(k_x,0)\right]^2 dk_x \tag{A31}$$

But by virtue of equation (A9)

$$\overline{E}_x^{(1)}(k_x,0) = \overline{E}_x^{(w)}(k_x,0) \tag{A32}$$

and

$$\overline{E}_x^{(w)}(k_x,0) = \int_{-a/2}^{a/2} \frac{V_o}{\sqrt{a}} e^{jk_x x}\, dx = \frac{2V_o}{\sqrt{a}} \frac{\sin\frac{k_x a}{2}}{k_x} \tag{A33}$$

Consequently, from equations (A1), (A31), (A32), and (A33), the admittance is found to be

$$Y = \frac{2}{\pi a}\int_{-\infty}^{\infty} \overline{Y}(k_x,0)\, \frac{\sin^2\frac{k_x a}{2}}{k_x^2}\, dk_x \tag{A34}$$

Equation (A34) is a particularly important result, since the admittance of the parallel-plate guide is now expressed as an integral over mode space and involving the spectral constant $\overline{Y}(k_x,0)$, which is dependent only on the nature of the external environment. Furthermore, since both $\overline{Y}(k_x,0)$ and its inverse transform

$$Y(x,0) = \frac{1}{2\pi}\int_{-\infty}^{\infty} \overline{Y}(k_x,0)\, e^{-jk_x x}\, dk_x \tag{A35}$$

are even functions of k_x and x, respectively, the integral in equation (A34) can be converted from mode space to physical space by use of the convolution theorem to give

$$Y = \frac{4}{a}\int_{-\infty}^{\infty} Y(x,0)\, F(x)\, dx \tag{A36}$$

where

$$F(x) = \frac{1}{2\pi}\int_{-\infty}^{\infty} \frac{\sin^2\frac{k_x a}{2}}{k_x^2}\, e^{-jk_x x}\, dk_x \tag{A37}$$

Application of residue theory to equation (A37) yields

$$\left.\begin{aligned} F(x) &= \tfrac{1}{4}(a - |x|) \qquad (|x| \leq a) \\ F(x) &= 0 \qquad\qquad\quad (|x| > a) \end{aligned}\right\} \tag{A38}$$

Thus, an alternate form for equation (A34) is

$$Y = \frac{2}{a}\int_0^a (a - x)\, Y(x)\, dx \tag{A39}$$

APPENDIX A

Equation (A39) may be more useful for purposes of numerical computations since the range of integration is finite.

For the problem under consideration

$$\overline{Y}(k_x,0) = \frac{\omega\epsilon_1}{k_{z,1}} \frac{U(k_x) + 1}{U(k_x) - 1} \tag{A40}$$

or

$$\overline{Y}(k_x,0) = \frac{\omega\epsilon_1}{k_{z,1}} \left(\frac{1 + j \dfrac{k_{z,2}\epsilon_1}{k_{z,1}\epsilon_2} \tan k_{z,1}d}{\dfrac{k_{z,2}\epsilon_1}{k_{z,1}\epsilon_2} + j \tan k_{z,1}d} \right) \tag{A41}$$

The inverse transform of equation (A41) is not readily evaluated except for certain special cases; consequently, in the spatial frequency domain the admittance is given by

$$Y = \frac{4}{\pi a} \int_0^\infty \frac{\sin^2 \dfrac{k_x a}{2}}{k_x^2} \left[\frac{\omega\epsilon_1}{k_{z,1}} \left(\frac{1 + j \dfrac{k_{z,2}\epsilon_1}{k_{z,1}\epsilon_2} \tan k_{z,1}d}{\dfrac{k_{z,2}\epsilon_1}{k_{z,1}\epsilon_2} + j \tan k_{z,1}d} \right) \right] dk_x \tag{A42}$$

which is the result given as equation (2). The surface wave propagation constants are then found by solving the equation

$$\frac{k_{z,2}\epsilon_1}{k_{z,1}\epsilon_2} + j \tan k_{z,1}d = 0 \tag{A43}$$

for the real roots of k_x.

APPENDIX B

LIMITING CASES

As a partial check on the analysis, equations (A41) and (A42) are compared with the following special cases, for which Y has previously been determined:

(1) Medium 1 a lossy dielectric and medium 2 free space – Under this condition equation (A41) becomes

$$\overline{Y}(k_x,0) = \frac{\omega\epsilon_1}{k_{z,1}} \frac{1 + j \dfrac{k_{z,2}\epsilon_1}{k_{z,1}\epsilon_0} \tan k_{z,1}d}{\dfrac{k_{z,2}\epsilon_1}{k_{z,1}\epsilon_0} + j \tan k_{z,1}d} \tag{B1}$$

where $k_{z,2} = \left(k_0^2 - k_x^2\right)^{1/2}$ with $k_0 = \omega\sqrt{\mu_0\epsilon_0}$, $\mathrm{Re}\left(k_{z,2}\right) > 0$, and $\mathrm{Im}\left(k_{z,2}\right) < 0$. This result is identical with the result established by Compton (ref. 3, pp. 39-40).

(2) Width d of medium 1 allowed to approach zero – For this case the external medium is a lossy half-space with the constitutive parameters μ_2 and ϵ_2. Under this condition equation (A41) approaches the value $\dfrac{\omega\epsilon_2}{k_{z,2}}$ and thus equation (A42) becomes

$$Y = \frac{4}{\pi a} \int_0^\infty \frac{\sin^2 \dfrac{k_x a}{2}}{k_x^2} \frac{\omega\epsilon_2}{k_{z,2}}\, dk_x \tag{B2}$$

Equation (B2) is the result established by Compton (ref. 3, p. 25). For this case $Y(x,0)$ is found to be (ref. 12, pp. 30-42)

$$Y(x,0) = \frac{1}{2\pi} \int_{-\infty}^{\infty} \frac{\omega\epsilon_2}{k_{z,2}} e^{-jk_x x}\, dk_x = \frac{\omega\epsilon_2}{2} H_0^{(2)}\left(k_2|x|\right) \tag{B3}$$

and thus, from equation (A40), the alternate form is

$$Y(x,0) = \frac{\omega\epsilon_2}{a} \int_0^a (a - x) H_0^{(2)}(k_2 x)\, dx \tag{B4}$$

(3) Dielectric constants of medium 1 and medium 2 equal – For this case the external environment is a semi-infinite dielectric with the constitutive parameters $\mu_1 = \mu_2$ and $\epsilon_1 = \epsilon_2$. Furthermore, as ϵ_1 approaches ϵ_2 and μ_1 approaches μ_2, the boundary effectively disappears; consequently, the admittance should reduce to the value given by equations (B2), (B3), and (B4), independently of d. This condition is evident from

examination of equation (A41). Note that, since $k_{z,1} = k_{z,2}$ for this case, the quantity in parentheses is equal to unity for any d, and hence

$$\overline{Y}(k_x,0) = \frac{\omega\epsilon_1}{k_{z,1}} = \frac{\omega\epsilon_2}{k_{z,2}}$$

as required.

(4) Medium 2 a perfect conductor – Under this condition the aperture is illuminating a perfectly conducting wall. For this case the imaginary part of ϵ_2 is infinite but

$$\frac{k_{z,2}}{\epsilon_2} = \frac{\left(k_2^2 - k_x^2\right)^{1/2}}{\epsilon_2} = \frac{\left(\omega^2\mu_2\epsilon_2 - k_x^2\right)^{1/2}}{\epsilon_2} \tag{B5}$$

or

$$\frac{k_{z,2}}{\epsilon_2} = \frac{\left[\left(\omega^2\mu_2\epsilon_2' - k_x^2\right) - j\omega^2\mu_2\epsilon_2''\right]^{1/2}}{\epsilon_2' - j\epsilon_2''} \tag{B6}$$

and as ϵ_2'' approaches infinity, the ratio $\frac{k_{z,2}}{\epsilon_2}$ approaches zero. As a result, equation (A41) becomes

$$\overline{Y}\, k_x,0 = -\frac{j\omega\epsilon_1}{k_{z,1} \tan k_{z,1}d} \tag{B7}$$

and equation (A42) becomes

$$Y = -\frac{4j}{\pi a}\int_0^\infty \frac{\sin^2 \frac{k_x a}{2}}{k_x^2} \frac{\omega\epsilon_1}{k_{z,1} \tan k_{z,1}d}\, dk_x \tag{B8}$$

which is in agreement with the result established by Jones and Swift (ref. 7, pp. 13-14), who have also converted this result to the alternate representation. For this case (ref. 7, pp. 31-35)

$$Y(x,0) = \frac{1}{2\pi}\int_{-\infty}^{\infty} \frac{-j\omega\epsilon_1}{k_{z,1} \tan k_{z,1}d} e^{-jk_x x}\, dk_x = \omega\epsilon_1 \sum_{n=0}^{\infty} \frac{e^{-j\gamma_n|x|}}{\left(1 + \delta_0^{\,n}\right)\gamma_n d} \tag{B9}$$

where

$$\gamma_n = \left[k_1^2 - \left(\frac{n\pi}{d}\right)^2\right]^{1/2} \qquad \left(\mathrm{Re}(\gamma_n) > 0;\ \ \mathrm{Im}(\gamma_n) \leq 0\right) \tag{B10}$$

Consequently

$$Y = \frac{2}{a}\int_0^a (a - x)\omega\epsilon_1 \sum_{n=0}^{\infty} \frac{e^{-j\gamma_n x}}{\left(1 + \delta_0^{\,n}\right)\gamma_n d}\, dx \tag{B11}$$

APPENDIX B

Equation (B11) is readily simplified to give

$$Y = \frac{2\omega\epsilon_1}{ad} \sum_{n=0}^{\infty} \left\{ \frac{1}{\left(1 + \delta_0{}^{n)}\right)\gamma_n{}^3} \left[\left(1 - \cos \gamma_n a\right) - j\left(\gamma_n a - \sin \gamma_n a\right) \right] \right\} \qquad \text{(B12)}$$

Physically, each of the n terms in equation (B12) represents the admittance presented to the aperture by the nth TM (to the X-axis) waveguide mode in medium 1; the γ_n in equation (B10) is the propagation constant for the nth mode.

APPENDIX C

NORMALIZATION OF THE ADMITTANCE EXPRESSION

For convenience in numerical computations, the results given in equations (A42) and (A43) can be normalized by letting

$$k_x = k_0\beta \tag{C1}$$

Then equation (A42) can be manipulated into the form

$$y = \frac{Y}{Y_0} = \frac{G + jB}{Y_0} = g + jb = \frac{2\epsilon_{r,1}}{\pi^2 a_\lambda}\int_0^\infty \frac{C(\beta)}{S_1(\beta)} f(\beta)\, d\beta \tag{C2}$$

where

$$\left.\begin{aligned} f(\beta) &= \frac{\sin^2 \frac{\beta A}{2}}{\beta^2} \qquad (\beta \neq 0) \\ f(\beta) &= (\pi a_\lambda)^2 \qquad (\beta = 0) \end{aligned}\right\} \tag{C3}$$

$$A = k_0 a = \frac{2\pi}{\lambda_0} a = 2\pi a_\lambda \tag{C4}$$

$$\frac{C(\beta)}{S_1(\beta)} = \frac{\epsilon_{r,2} \cos DS_1(\beta) + j\epsilon_{r,1} DS_2(\beta) \frac{\sin DS_1(\beta)}{DS_1(\beta)}}{\epsilon_{r,1} S_2(\beta) \cos DS_1(\beta) + j\epsilon_{r,2} S_1(\beta) \sin DS_1(\beta)} \tag{C5}$$

$$D = k_0 d = \frac{2\pi}{\lambda_0} d = 2\pi d_\lambda \tag{C6}$$

$$S_i(\beta) = \left(N_i^2 - \beta^2\right)^{1/2} \qquad \left(\mathrm{Re}\left[S_i(\beta)\right] > 0;\ \ \mathrm{Im}\left[S_i(\beta)\right] \leq 0\right) \tag{C7}$$

$$N_i^2 = \mu_{r,i}\epsilon_{r,i} \tag{C8}$$

$$\epsilon_{r,i} = \epsilon'_{r,i} - j\epsilon''_{r,i} = \frac{\epsilon_i}{\epsilon_0} = \frac{\epsilon'_i}{\epsilon_0} - j\frac{\epsilon''_i}{\epsilon_0} \tag{C9}$$

$$\mu_{r,i} = \frac{\mu_i}{\mu_0} \tag{C10}$$

and, in normalized form, the surface wave poles correspond to the real values of β satisfying the equation

$$\tan DS_1(\beta) = j \frac{\epsilon_{r,2} S_1(\beta)}{\epsilon_{r,1} S_2(\beta)} \tag{C11}$$

The results given in equations (C2) to (C11) can be further simplified and applied to the problem of interest in this paper by assuming that both medium 1 and medium 2 are lossless $\left(\epsilon''_{r,1} = \epsilon''_{r,2} = 0\right)$, nonmagnetic $\left(\mu_{r,1} = \mu_{r,2} = 1\right)$ dielectrics where $\epsilon'_{r,2} \geq \epsilon'_{r,1} \geq 1$; that is, $N_2 \geq N_1$. An examination of equation (C11) under these conditions reveals that no surface waves are excited in the dielectric layer. Then by use of equation (C7) in equations (C2) and (C5) the admittance can be written in the form given by equations (3) to (12).

For the aperture radiating into a lossless dielectric half-space, equation (B4) is given in normalized form as

$$y = 2\pi\epsilon_r \int_0^{a_\lambda} \left(1 - \frac{x_\lambda}{a_\lambda}\right) H_0^{(2)}\left(2\pi\sqrt{\epsilon_r}\, x_\lambda\right) dx_\lambda \tag{C12}$$

This result is used to obtain the computations in figure 4.

REFERENCES

1. Burnside, Walter Dennis: The Reflection Coefficient of a TEM Mode Symmetric Parallel-Plate Waveguide Illuminating a Lossless Dielectric Layer. Rep. 1691-25 (NASA Grant No. NsG-448), ElectroScience Lab., Ohio State Univ., May 1, 1968.

2. Rudduck, R. C.: Application of Wedge Diffraction to Antenna Theory. NASA CR-372, 1966.

3. Compton, R. T., Jr.: The Admittance of Aperture Antennas Radiating Into Lossy Media. Rep. 1691-5 (NASA Grant No. NsG-448), Antenna Lab., Ohio State Univ. Res. Found., Mar. 15, 1964.

4. Galejs, Janis; and Mentzoni, Michael H.: Waveguide Admittance for Radiation Into Plasma Layers – Theory and Experiment. IEEE Trans. Antennas Propagation, vol. AP-15, no. 3, May 1967, pp. 465-470.

5. Croswell, William F.; Rudduck, Roger C.; and Hatcher, Douglas M.: The Admittance of a Rectangular Waveguide Radiating Into a Dielectric Slab. IEEE Trans. Antennas Propagation, vol. AP-15, no. 5, Sept. 1967, pp. 627-633.

6. Bailey, Marion C.; and Swift, Calvin T.: Input Admittance of a Circular Waveguide Aperture Covered by a Dielectric Slab. IEEE Trans. Antennas Propagation, vol. AP-16, no. 4, July 1968, pp. 386-391.

7. Jones, J. Earl; and Swift, C. T.: The Aperture Admittance of a Ground-Plane-Mounted Waveguide Illuminating a Perfectly Conducting Sheet. NASA TN D-4366, 1968.

8. Jones, J. Earl; Tsai, L. L.; Rudduck, R. C.; Swift, C. T.; and Burnside, W. D.: The Admittance of a Parallel-Plate Waveguide Aperture Illuminating a Metal Sheet. IEEE Trans. Antennas Propagation, vol. AP-16, no. 5, Sept. 1968, pp. 528-535.

9. Fante, Ronald L.: The Effect of an Offset Impedance Sheet on the Admittance of a Slot Antenna. IEEE Trans. Antennas Propagation, vol. AP-15, no. 4, July 1967, pp. 516-518.

10. Ghose, Rabindra N.: Microwave Circuit Theory and Analysis. McGraw-Hill Book Co., Inc., 1963.

11. Harrington, Roger F.: Time-Harmonic Electromagnetic Fields. McGraw-Hill Book Co., Inc., 1961.

12. Compton, R. T., Jr.: The Aperture Admittance of a Rectangular Waveguide Radiating Into a Lossy Half-Space. Rep. 1691-1 (NASA Grant No. NsG-448), Antenna Lab., Ohio State Univ., Sept. 30, 1963.

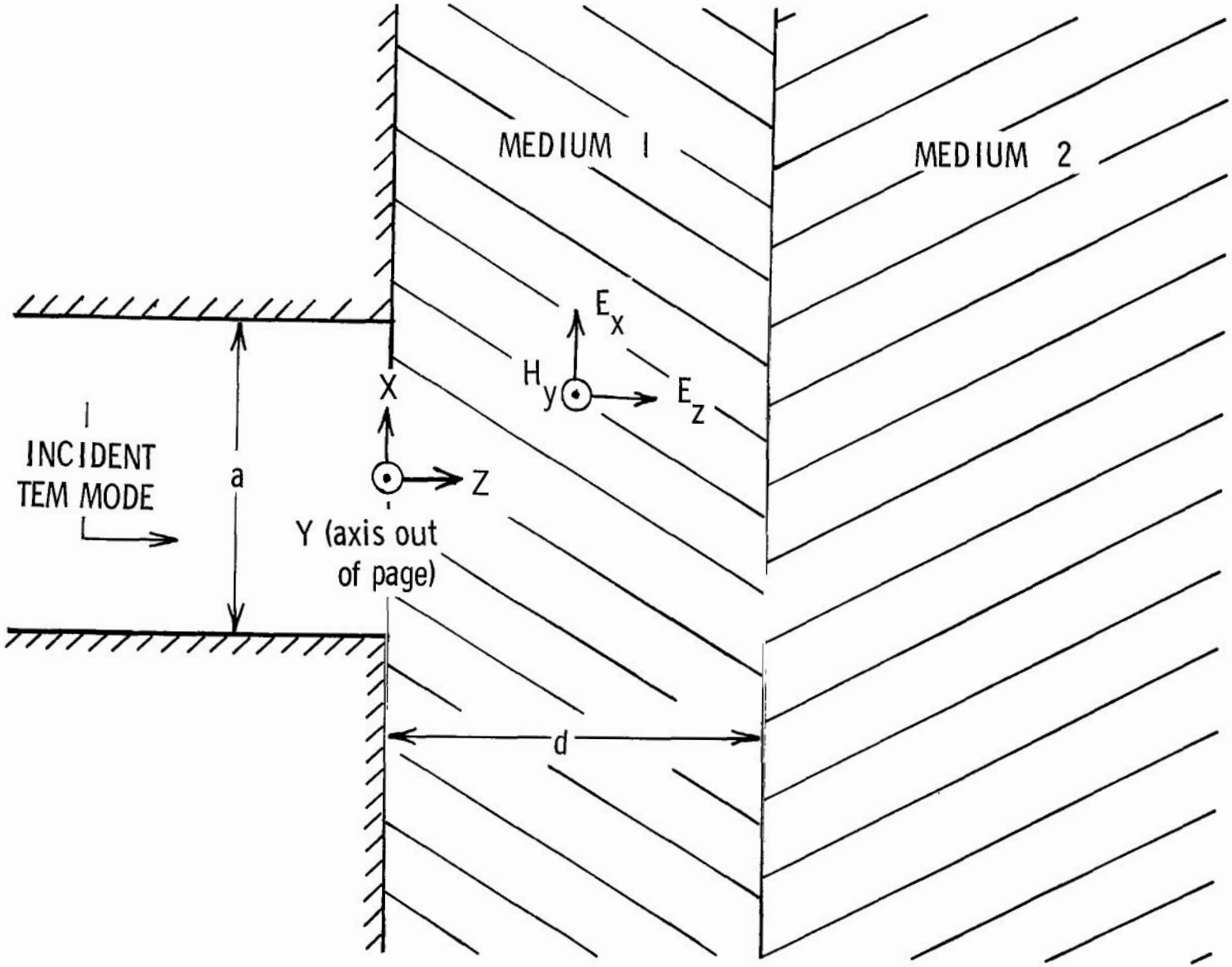

Figure 1.- Parallel-plate aperture illuminating dielectric-dielectric boundary, displaced distance d.

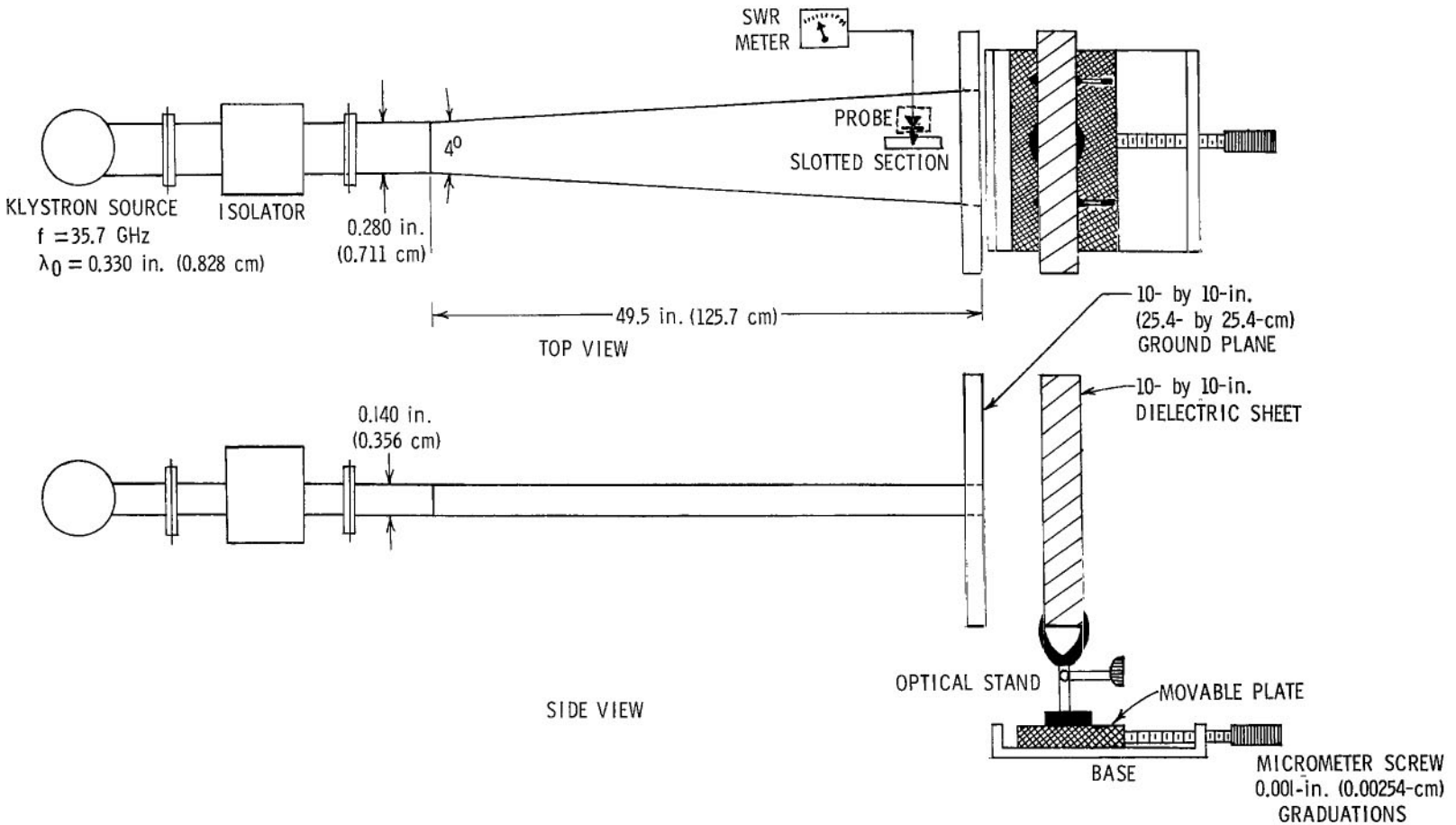

Figure 2.- Experimental apparatus.

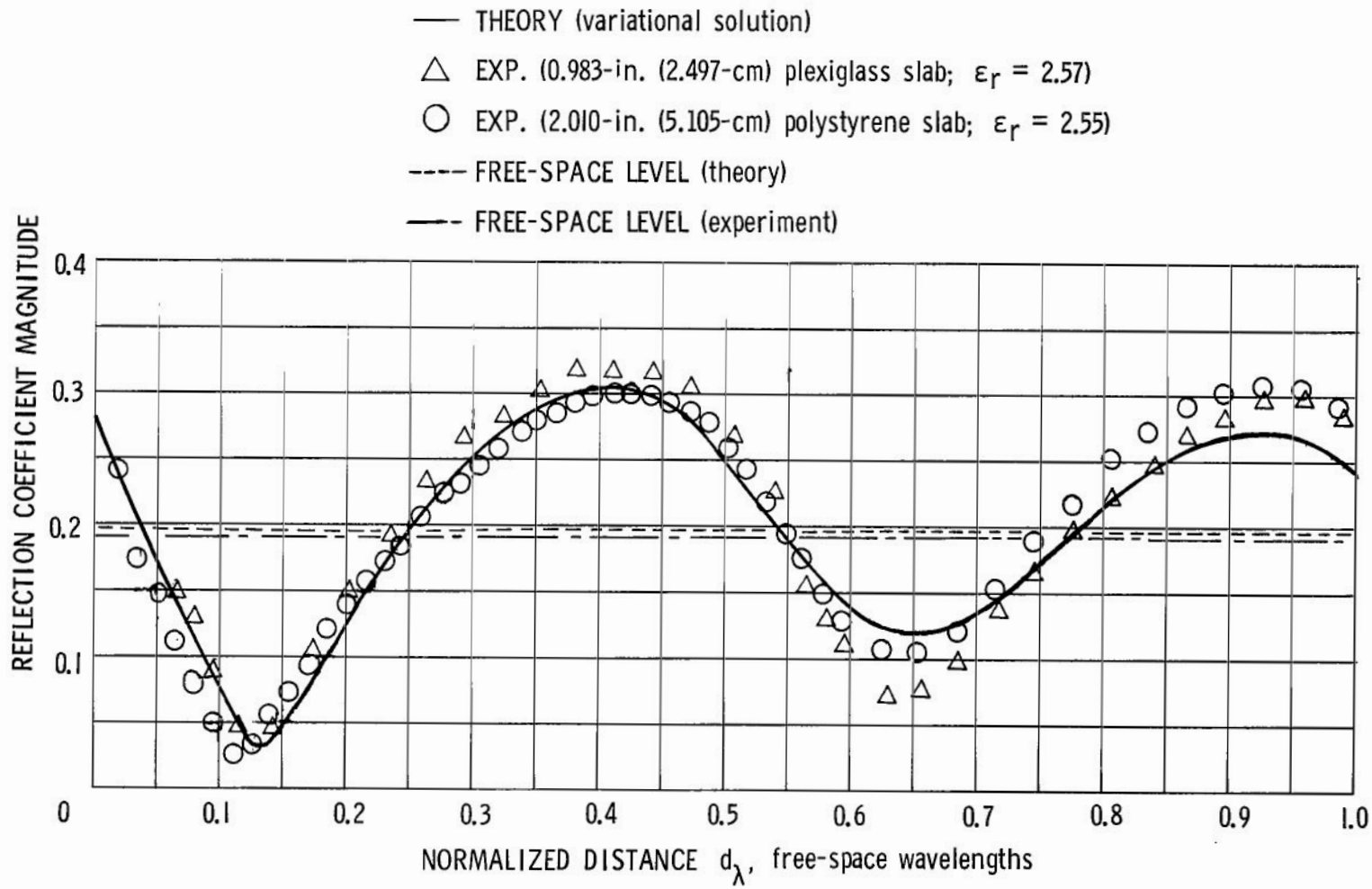

Figure 3.- Comparison of theory and experiment for reflection coefficient magnitude as a function of width of medium 1.

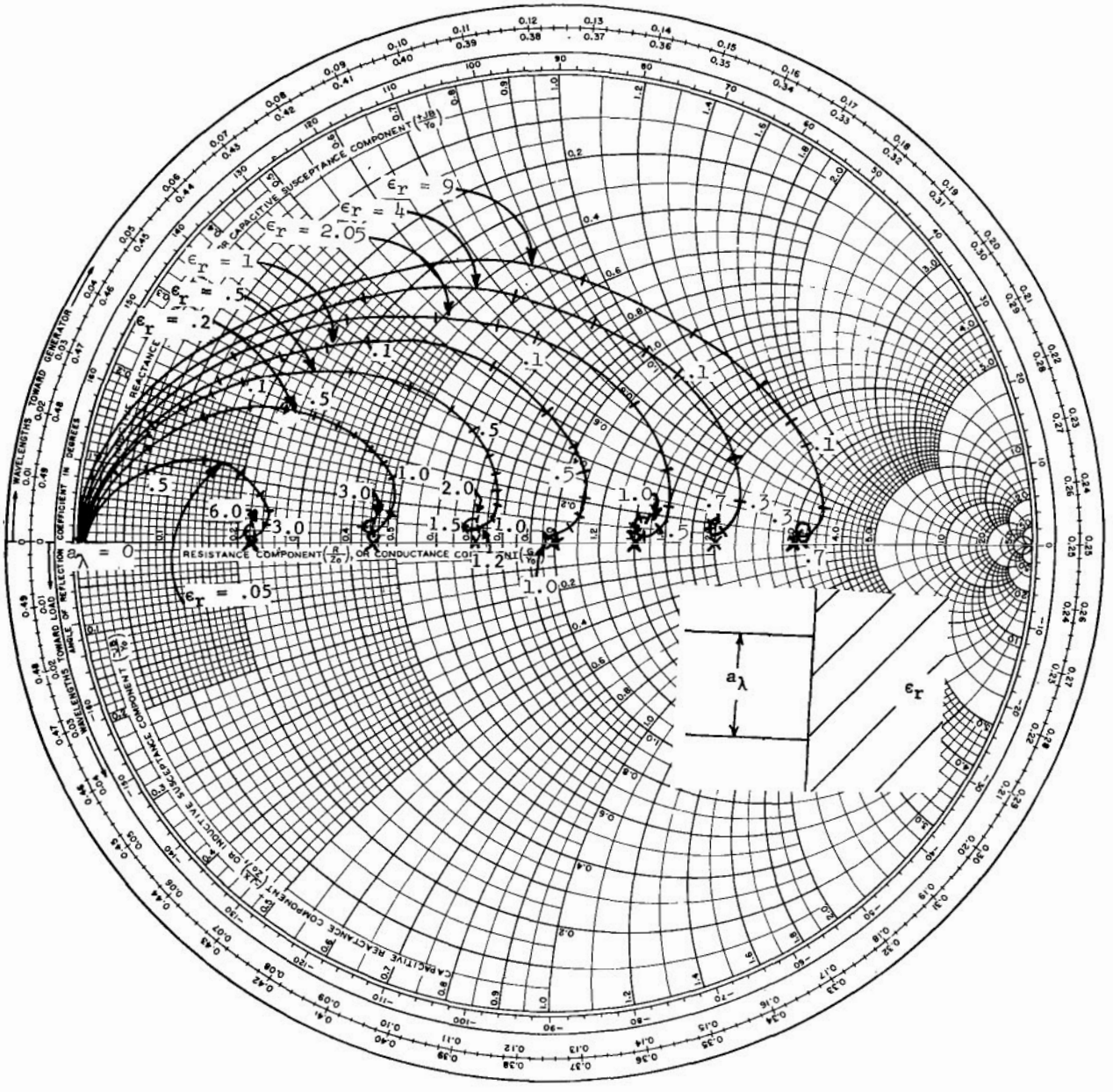

Figure 4.- Admittance of TEM mode parallel-plate aperture radiating into half-space.

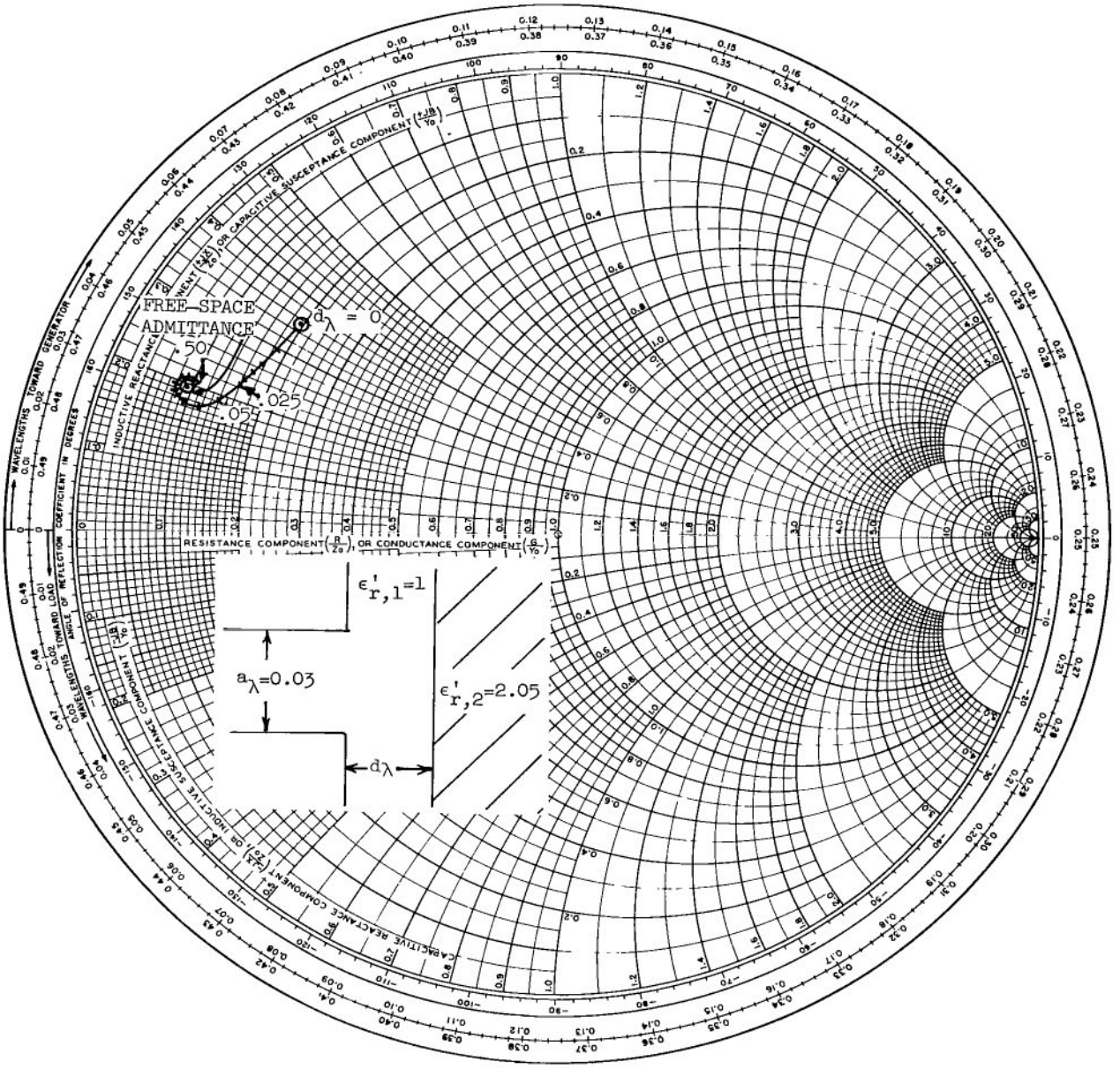

(a) $\epsilon'_{r,2} = 2.05$.

Figure 5.- Normalized aperture admittance of ground-plane-mounted, parallel-plate waveguide illuminating an air-dielectric boundary.

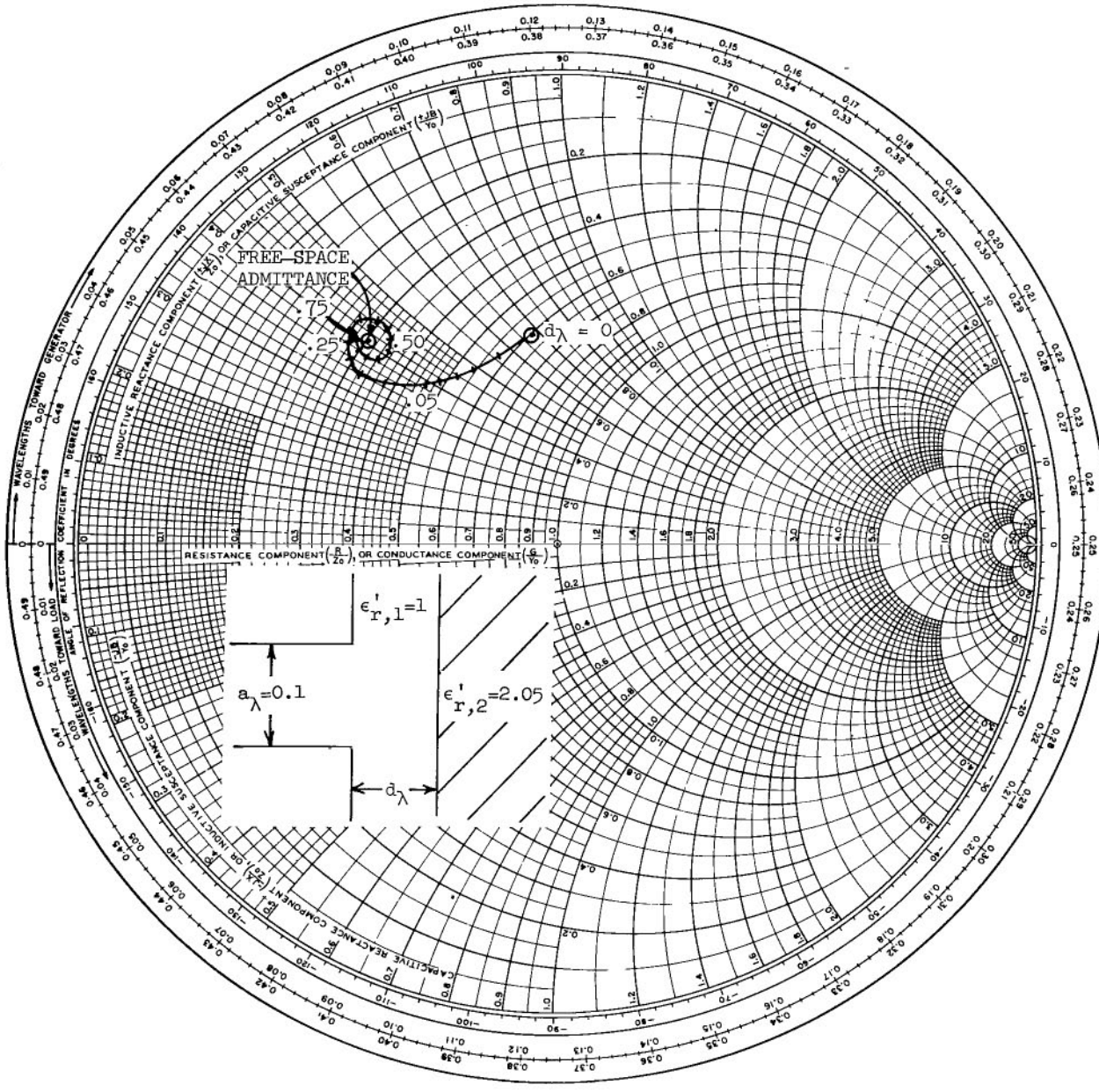

(a) $\epsilon'_{r,2} = 2.05$. Continued.

Figure 5.- Continued.

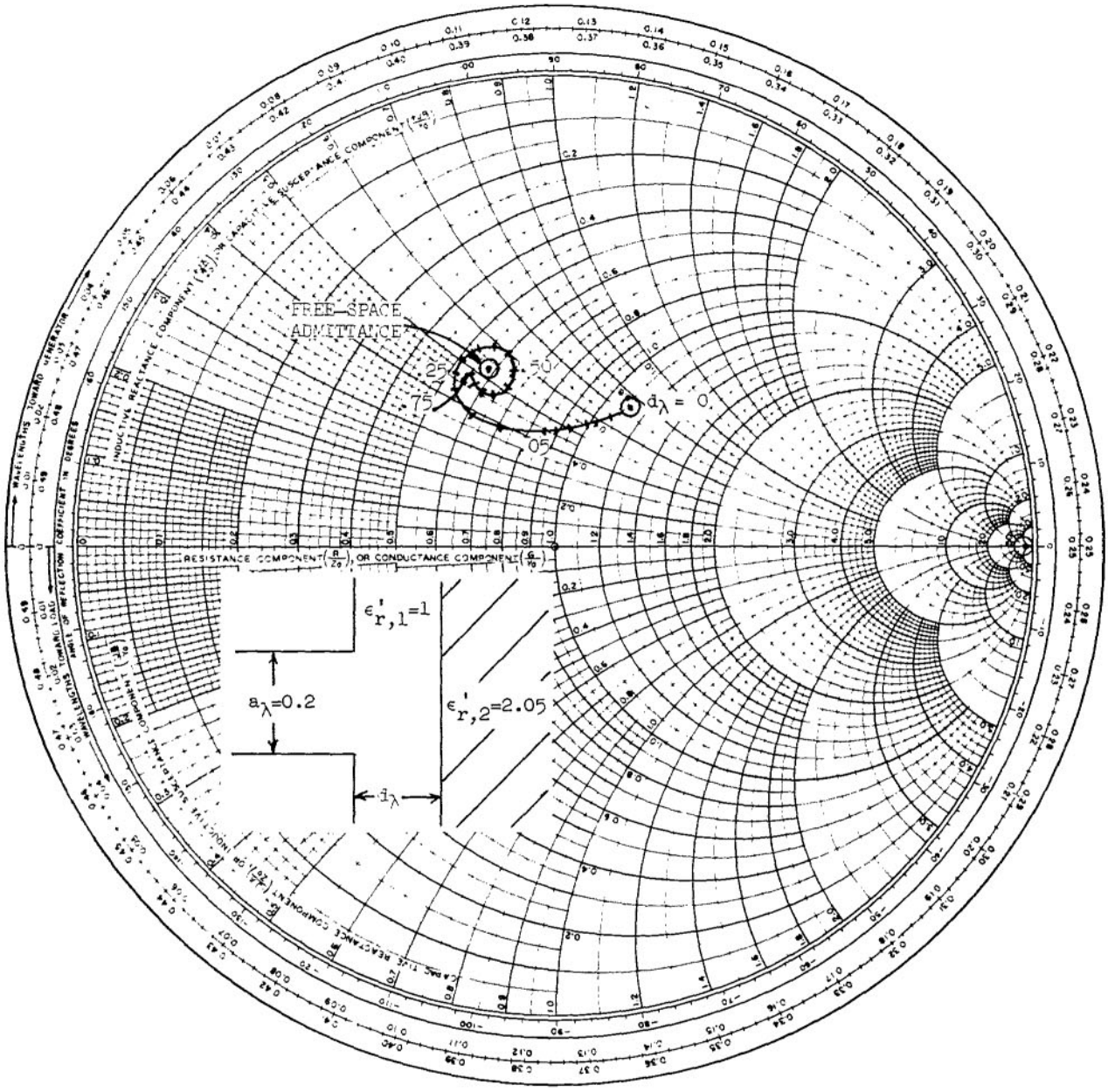

(a) $\epsilon'_{r,2} = 2.05$. Continued.

Figure 5.- Continued.

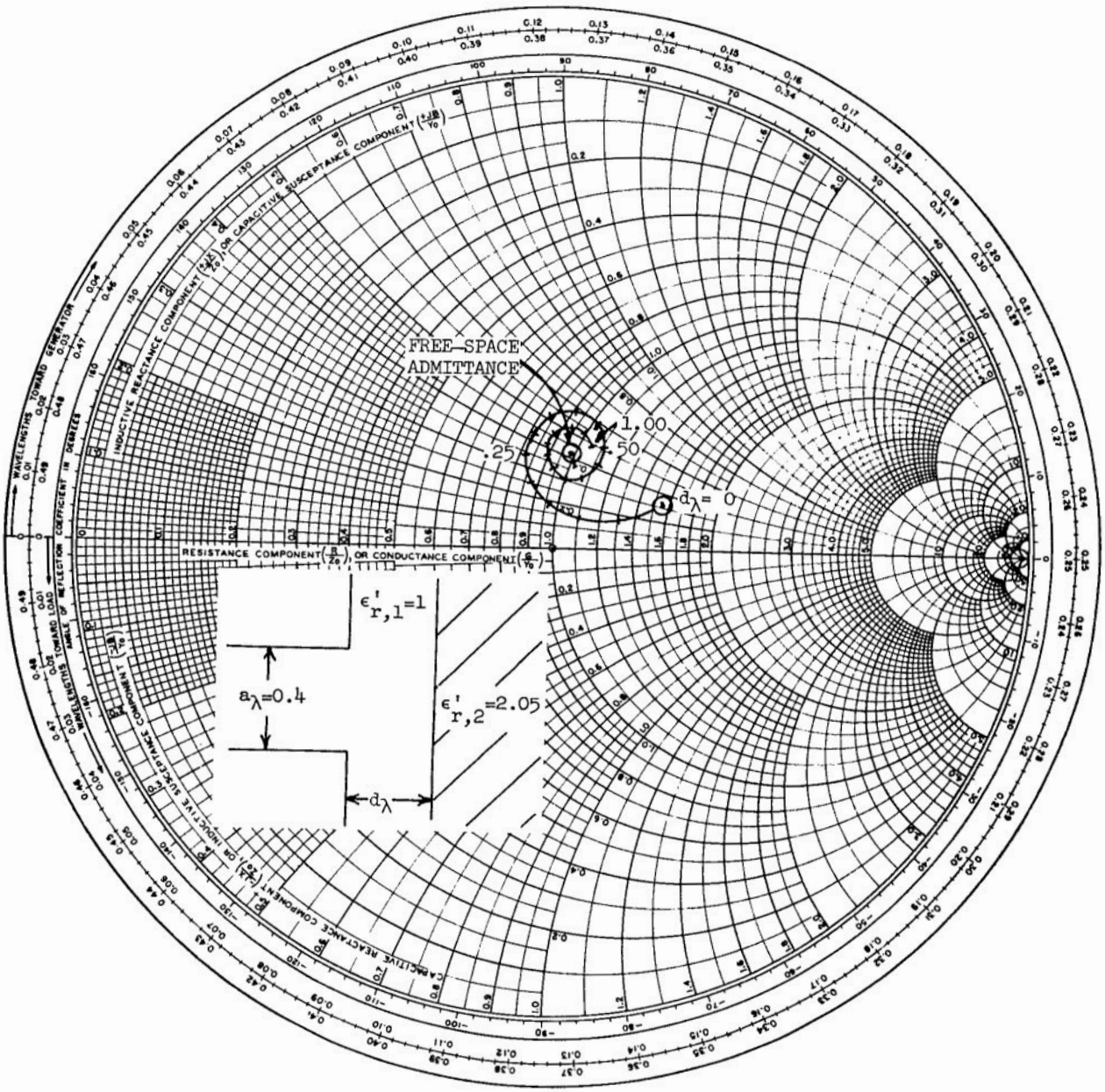

(a) $\epsilon'_{r,2} = 2.05$. Continued.

Figure 5.- Continued.

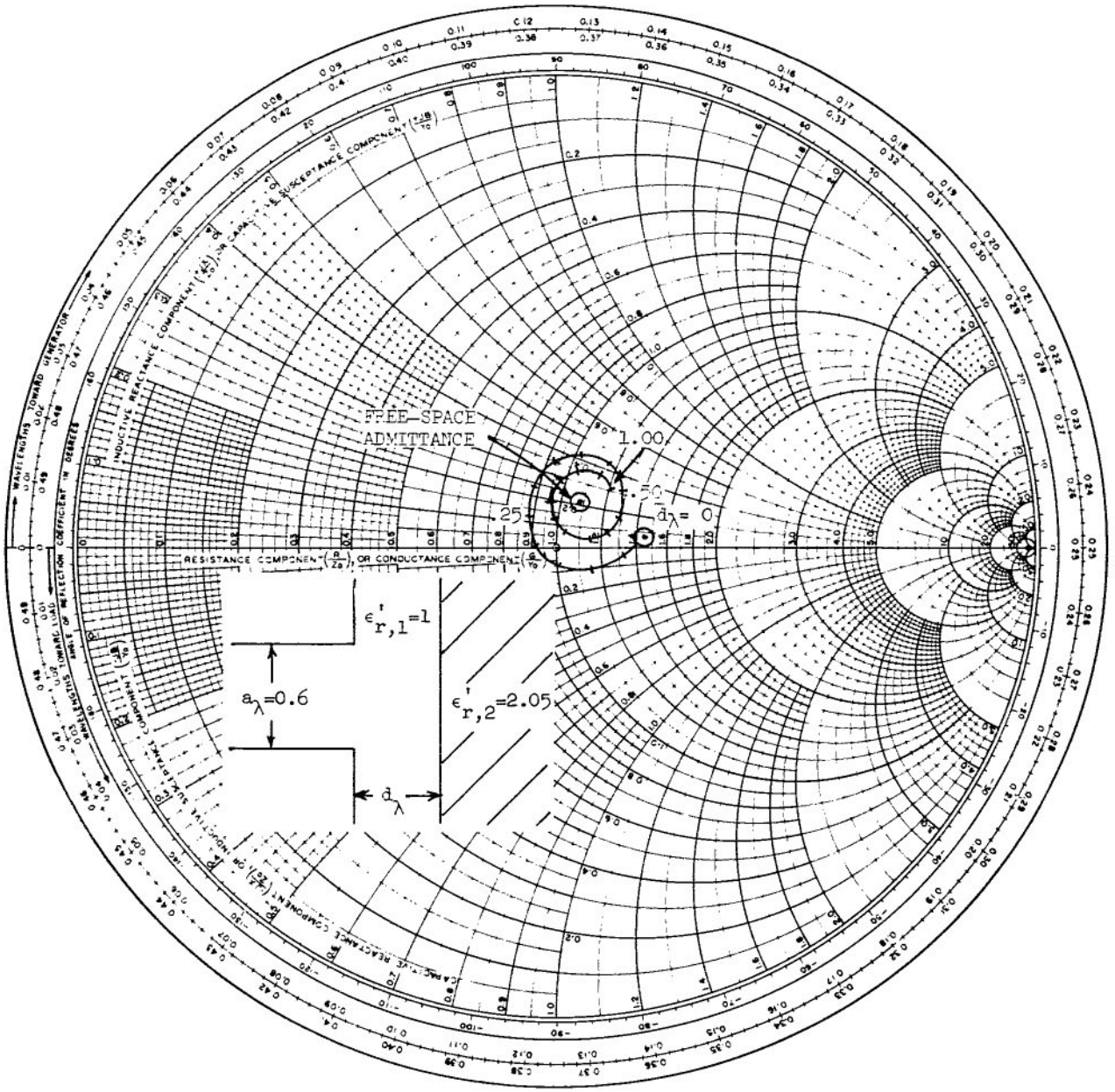

(a) $\epsilon'_{r,2}$ = 2.05. Concluded.

Figure 5.- Continued.

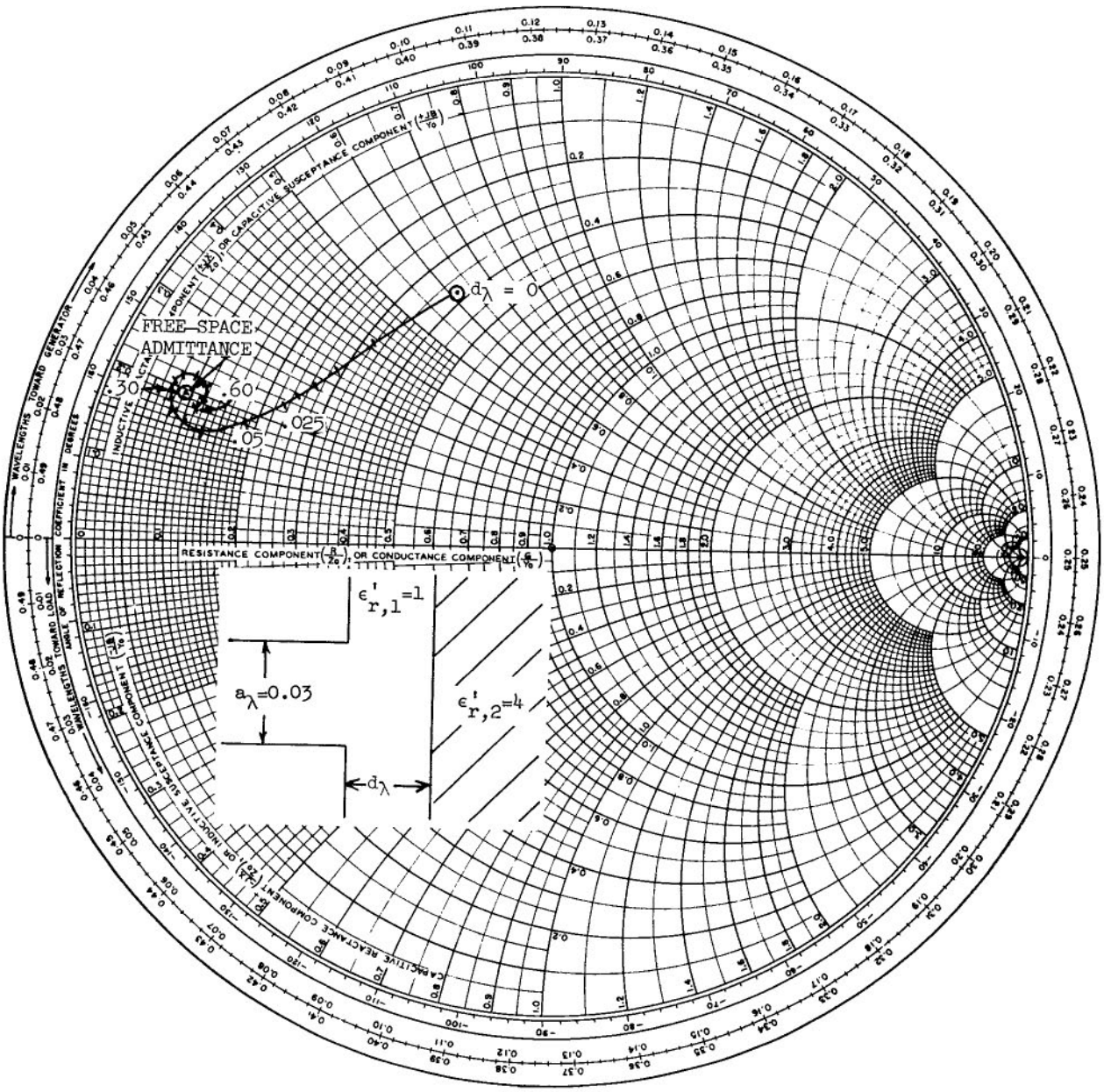

(b) $\epsilon'_{r,2} = 4$.

Figure 5.- Continued.

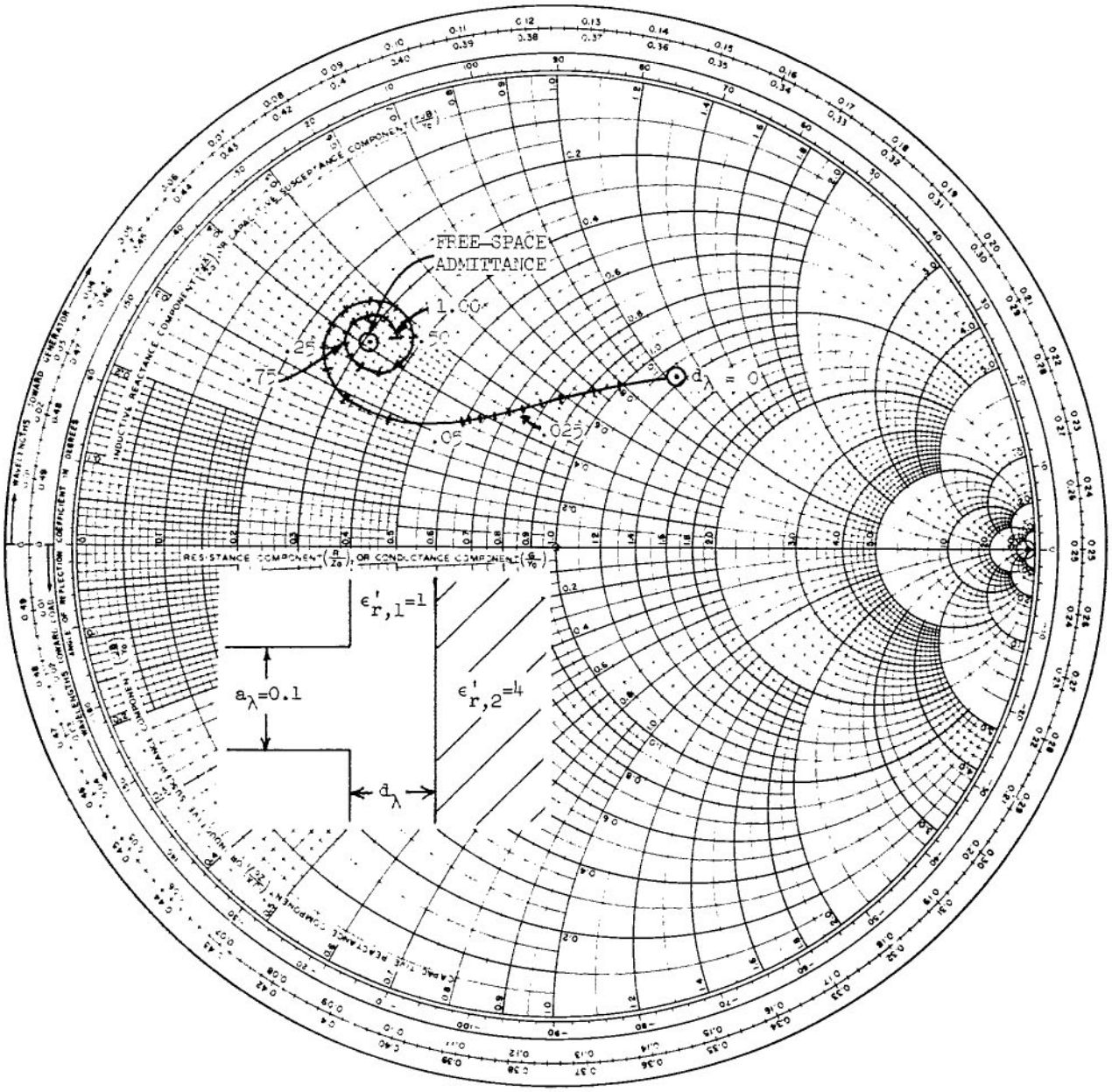

(b) $\varepsilon'_{r,2} = 4$. Continued.

Figure 5.- Continued.

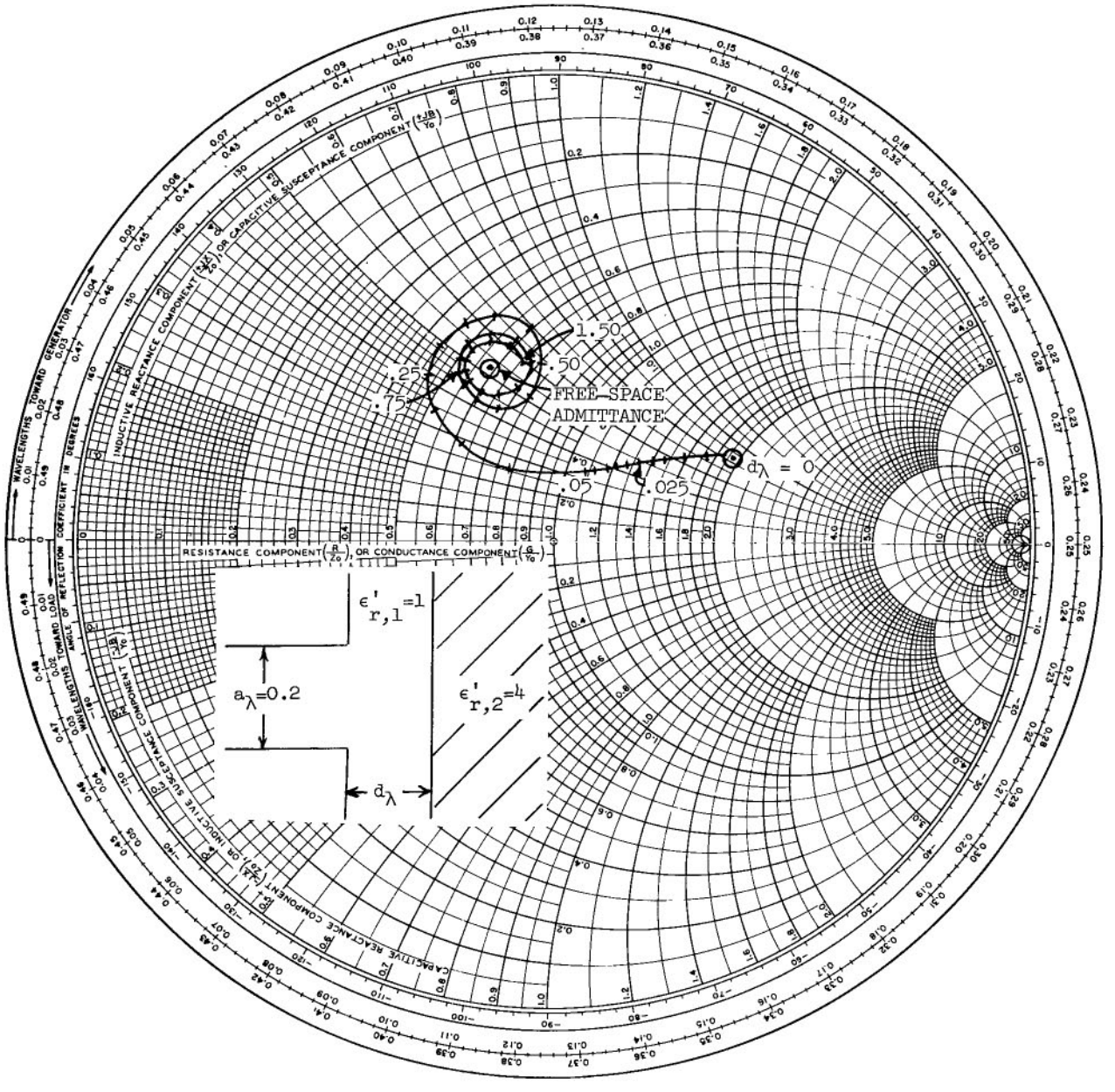

(b) $\epsilon'_{r,2} = 4$. Continued.

Figure 5.- Continued.

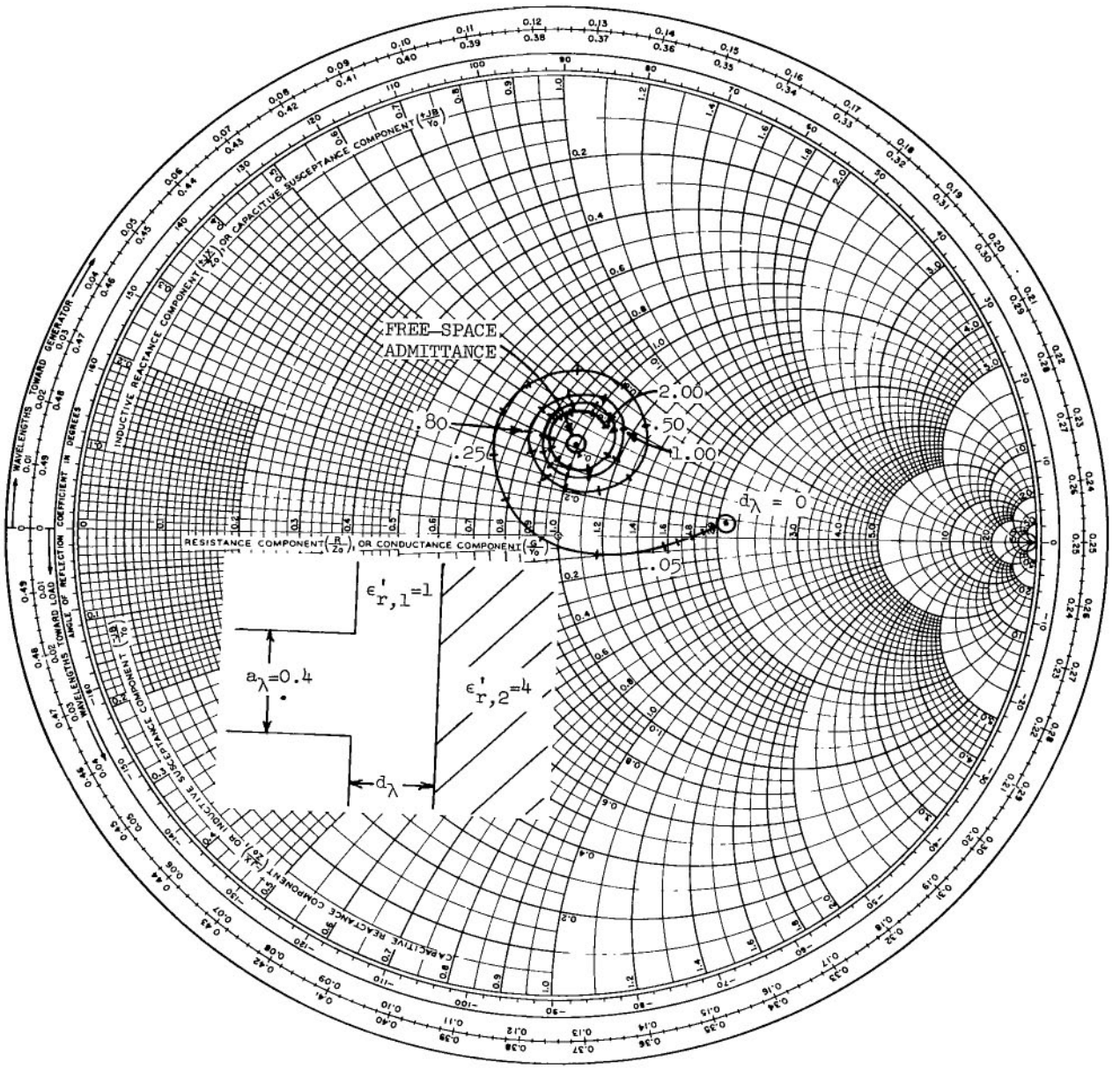

(b) $\epsilon'_{r,2} = 4$. Continued.

Figure 5.- Continued.

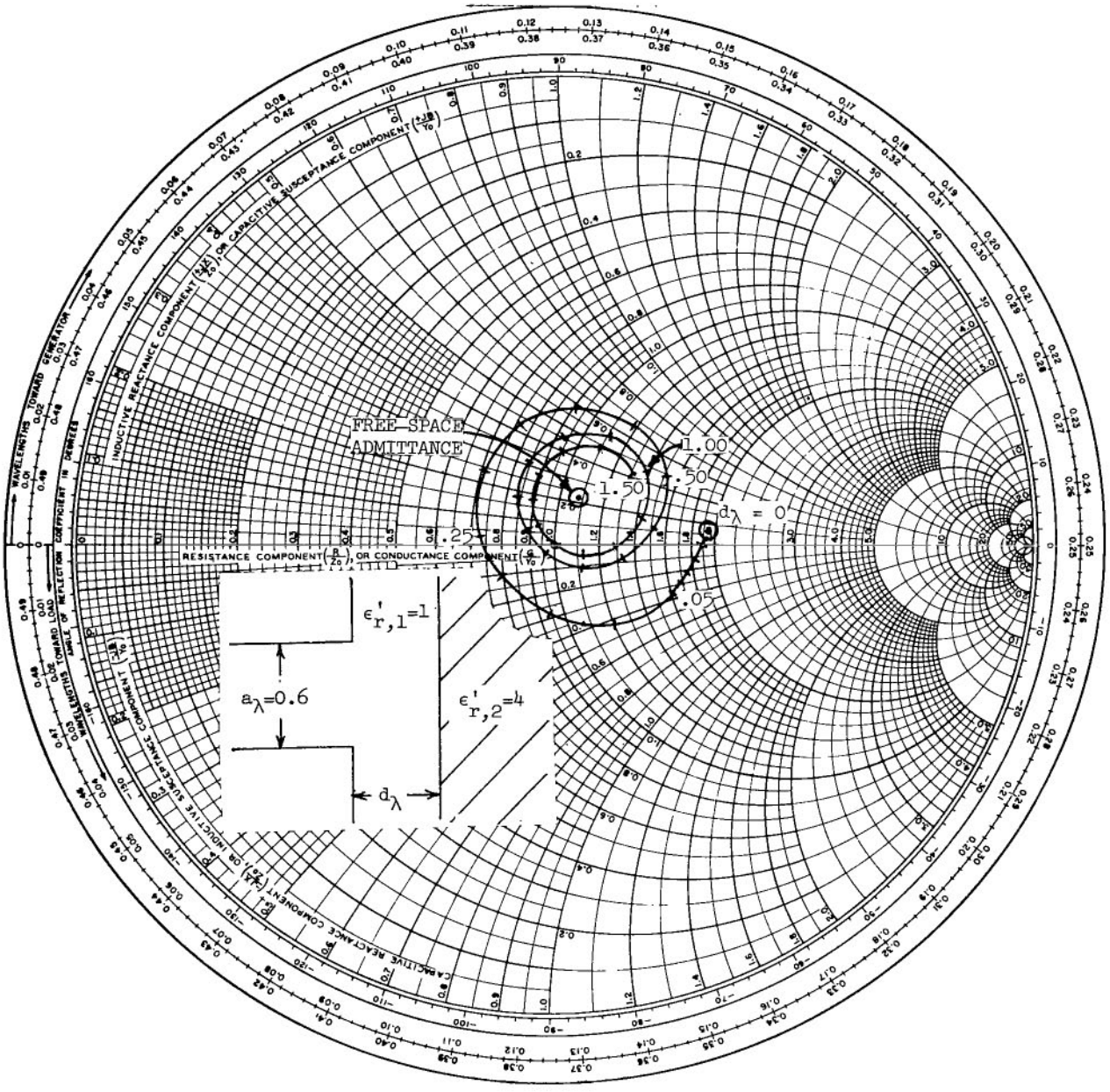

(b) $\epsilon'_{r,2} = 4$. Concluded.

Figure 5.- Continued.

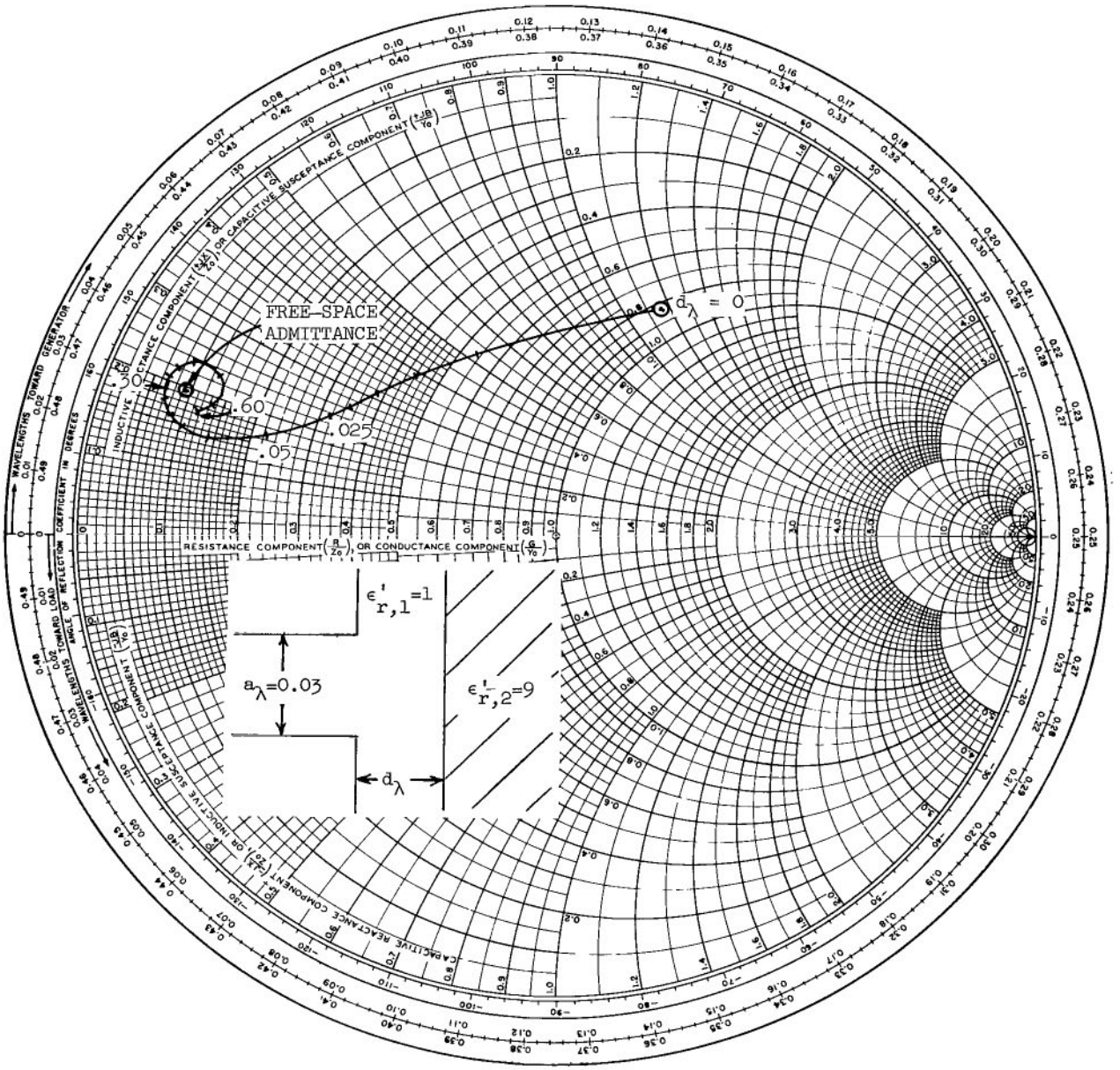

(c) $\epsilon'_{r,2} = 9$.

Figure 5.- Continued.

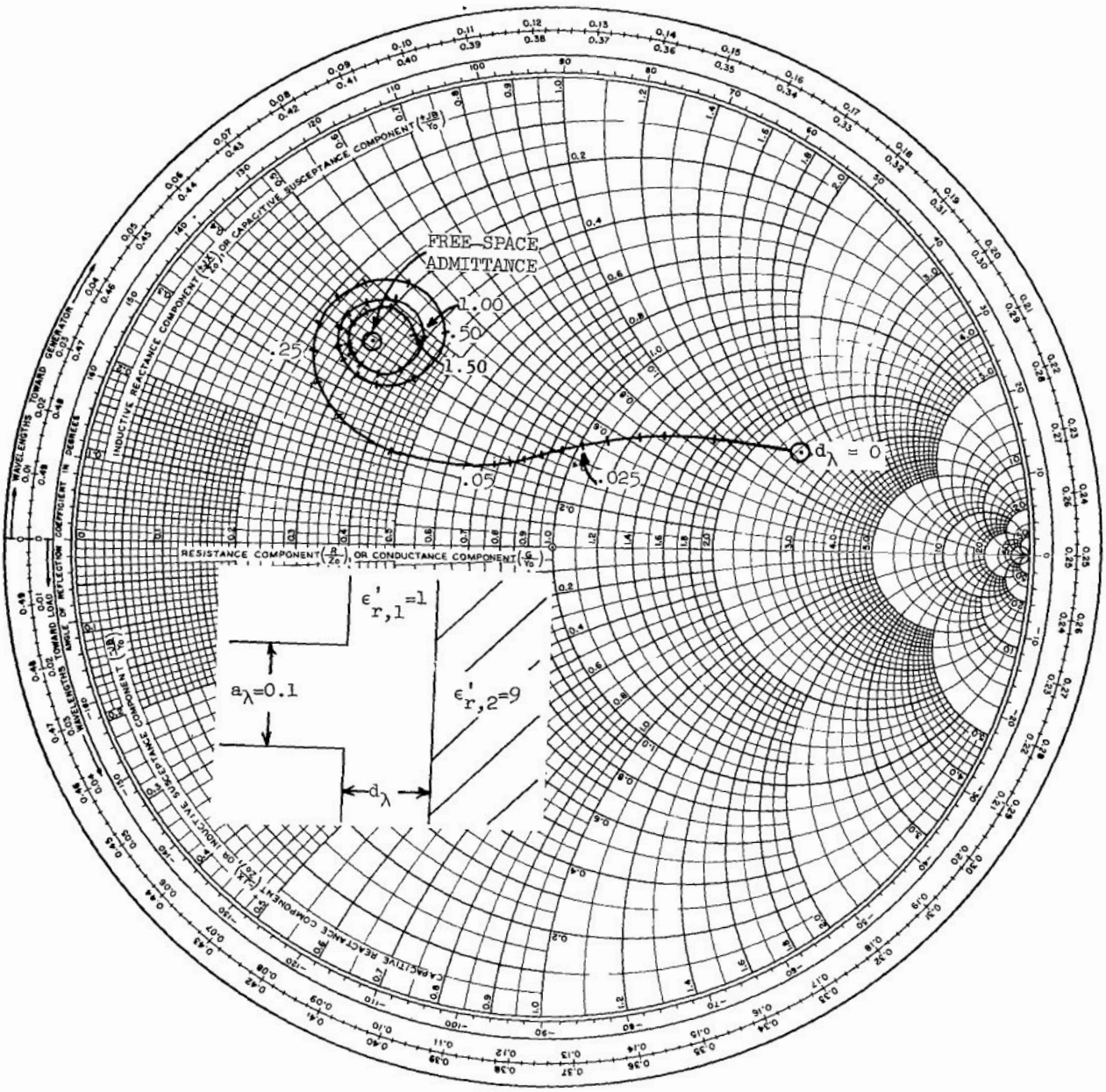

(c) $\epsilon'_{r,2} = 9$. Continued.

Figure 5.- Continued.

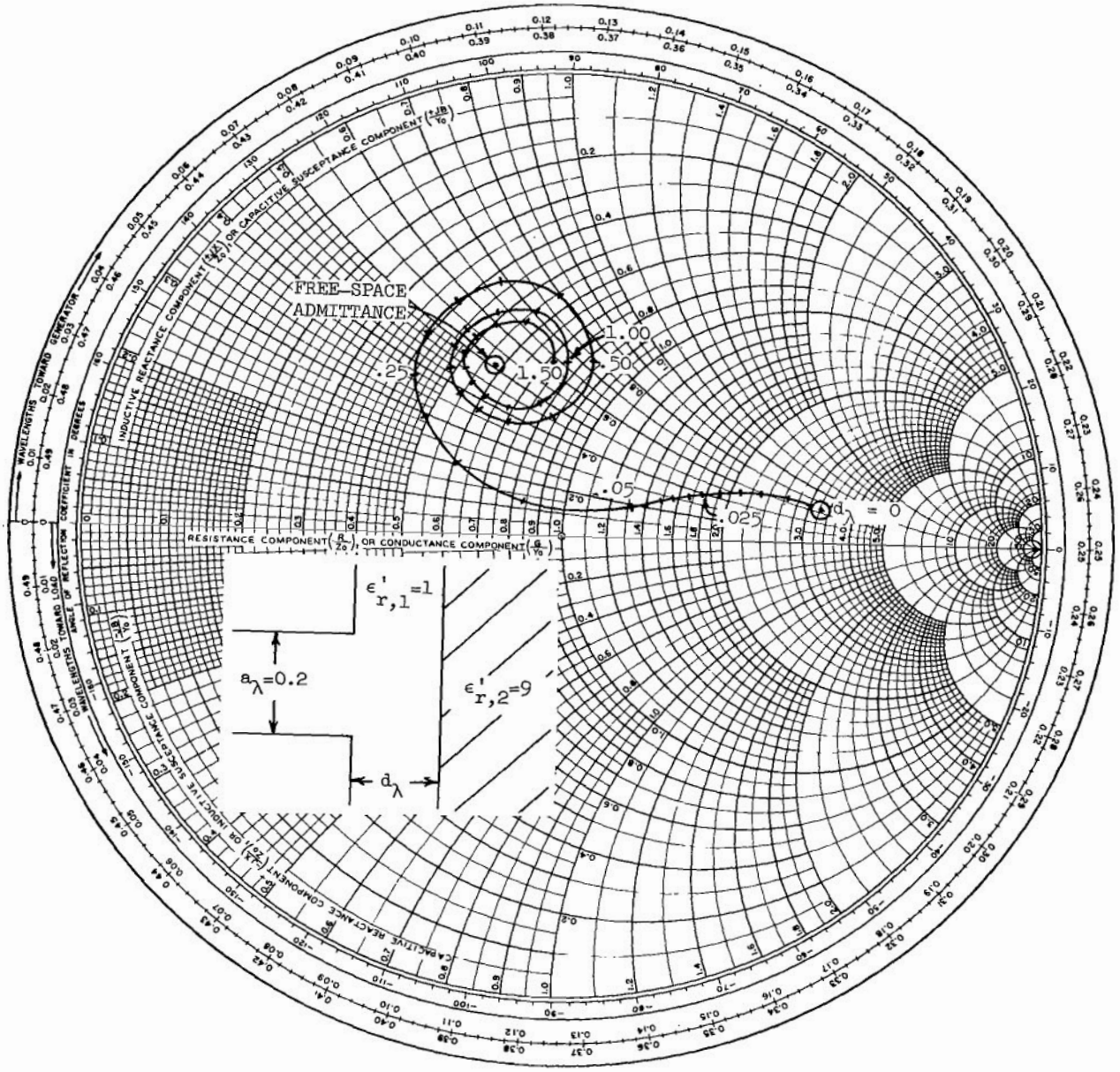

(c) $\epsilon'_{r,2} = 9$. Continued.

Figure 5.- Continued.

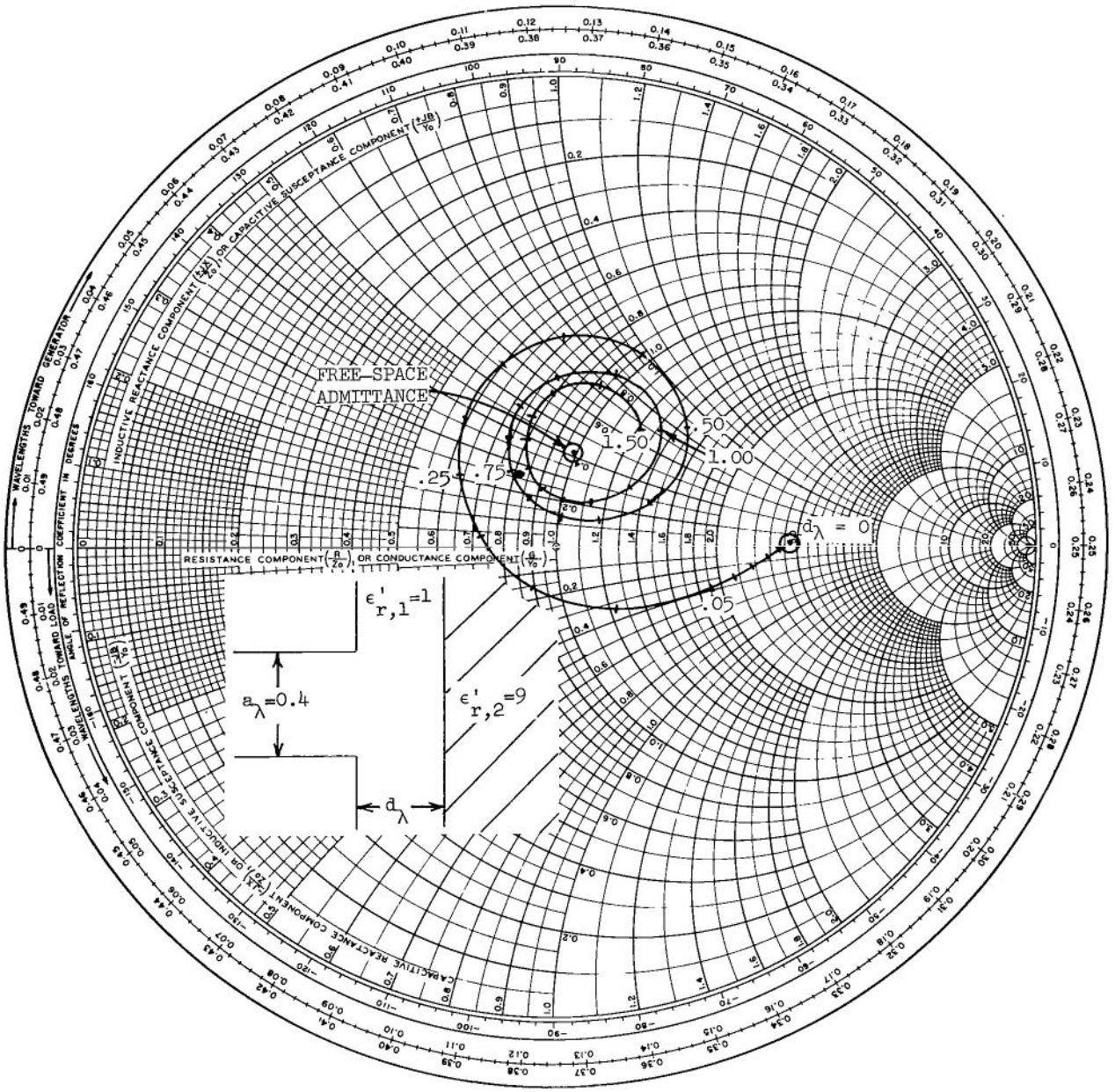

(c) $\epsilon'_{r,2} = 9$. Continued.

Figure 5.- Continued.

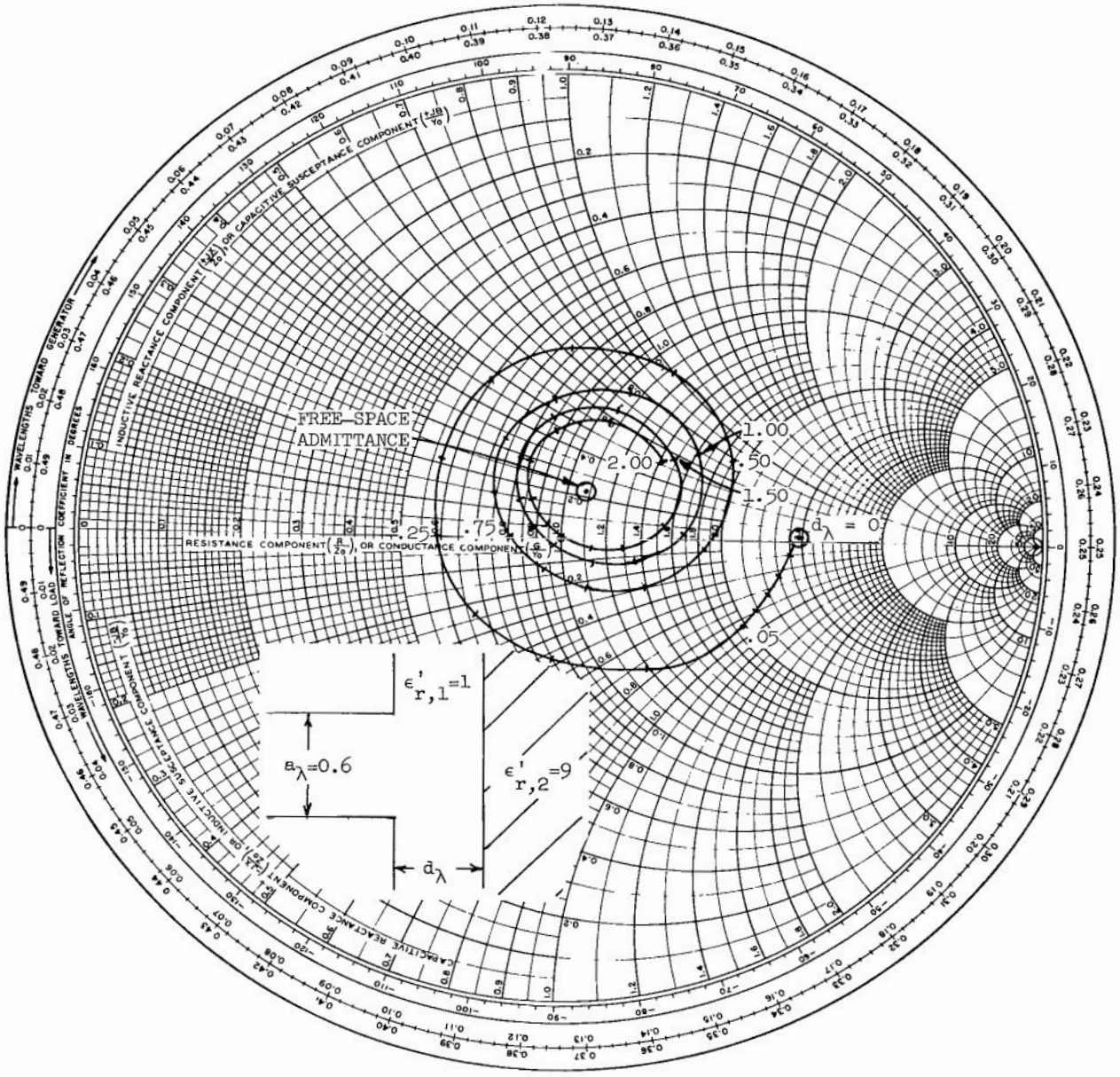

(c) $\epsilon'_{r,2} = 9$. Concluded.

Figure 5.- Concluded.

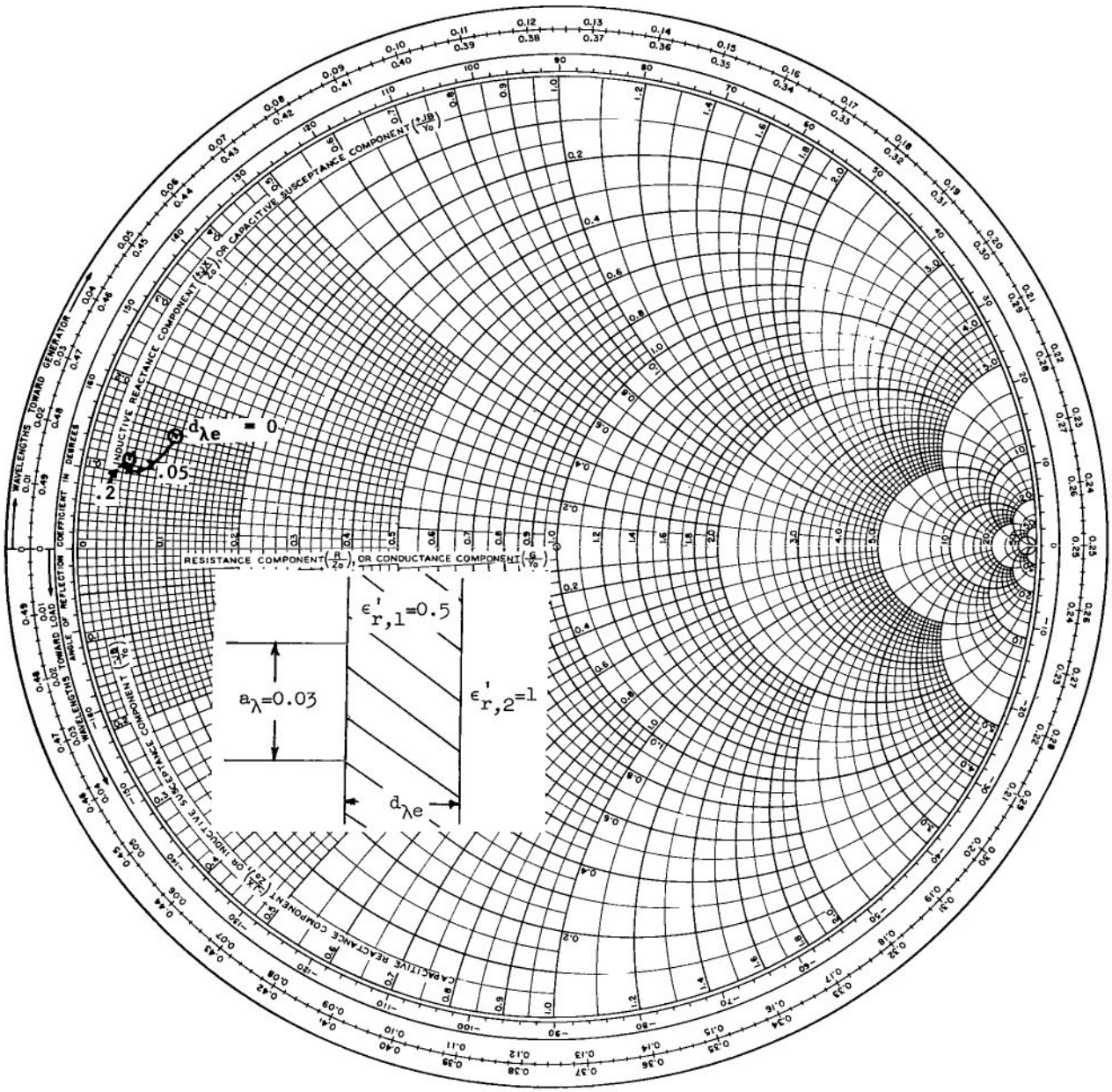

(a) $\epsilon'_{r,1} = 0.5$.

Figure 6.- Normalized aperture admittance of ground-plane-mounted, parallel-plate waveguide coated with an underdense plasma.

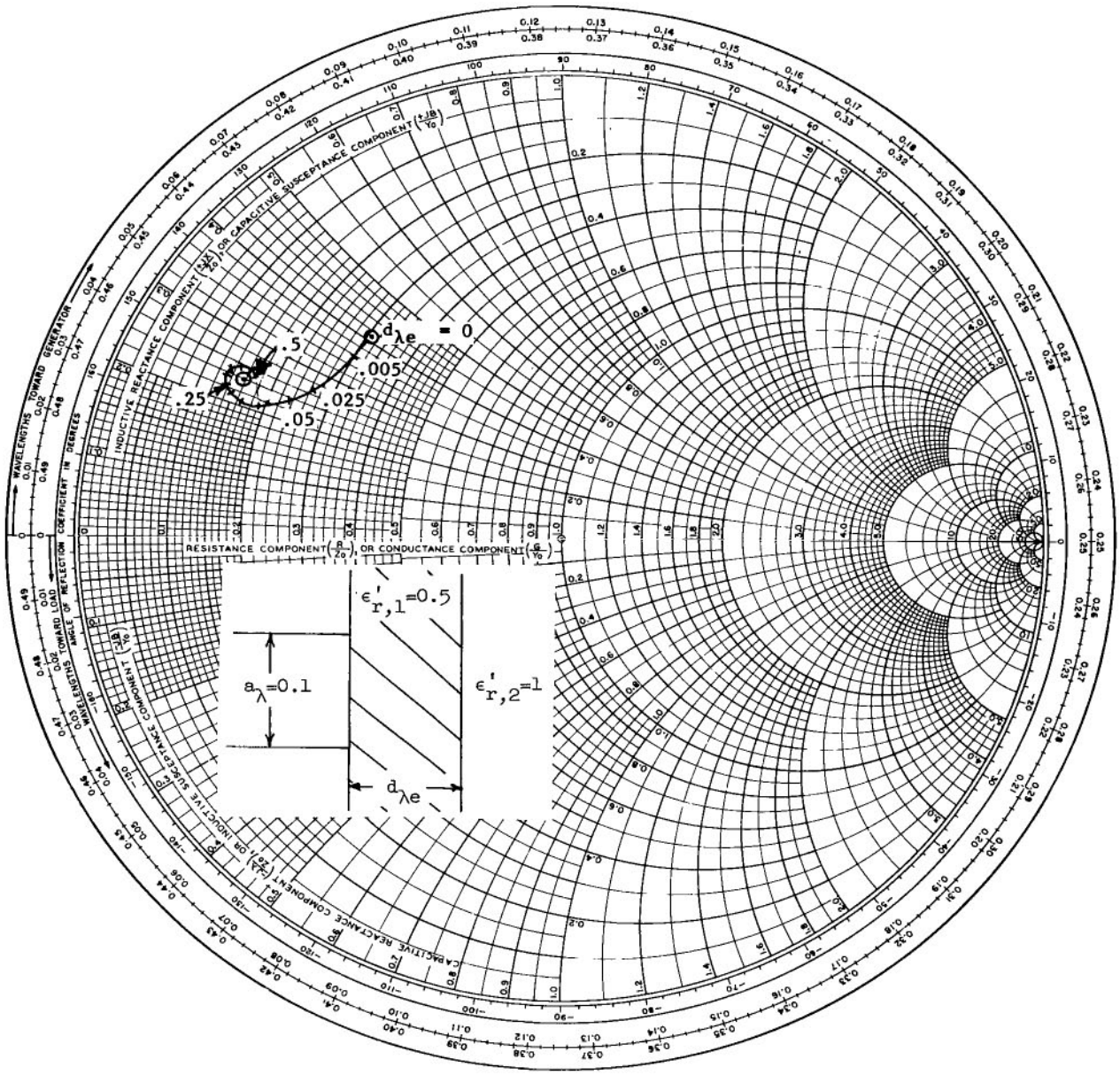

(a) $\epsilon'_{r,1}$ = 0.5. Continued.

Figure 6.- Continued.

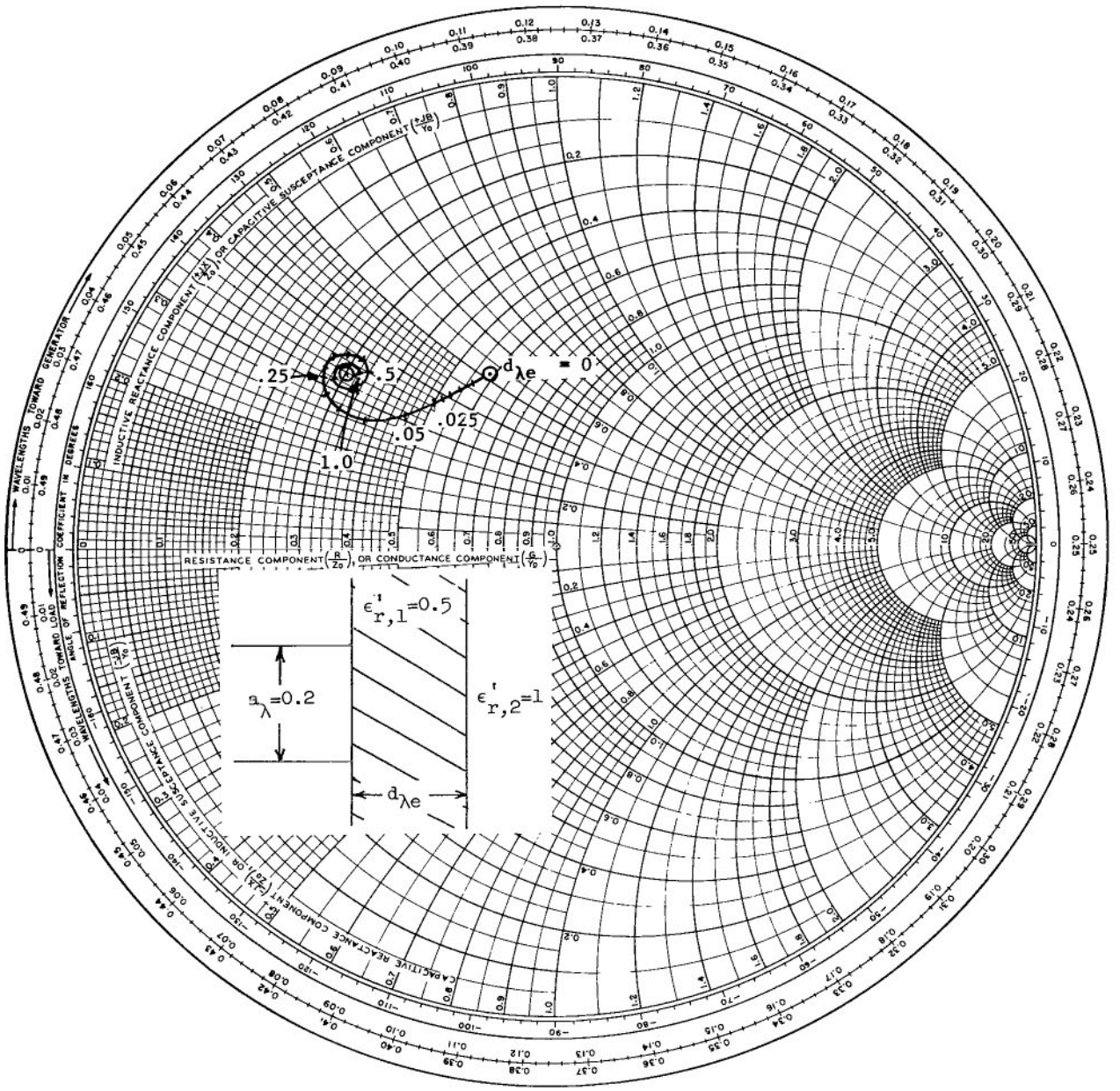

(a) $\epsilon'_{r,1} = 0.5$. Continued.

Figure 6.- Continued.

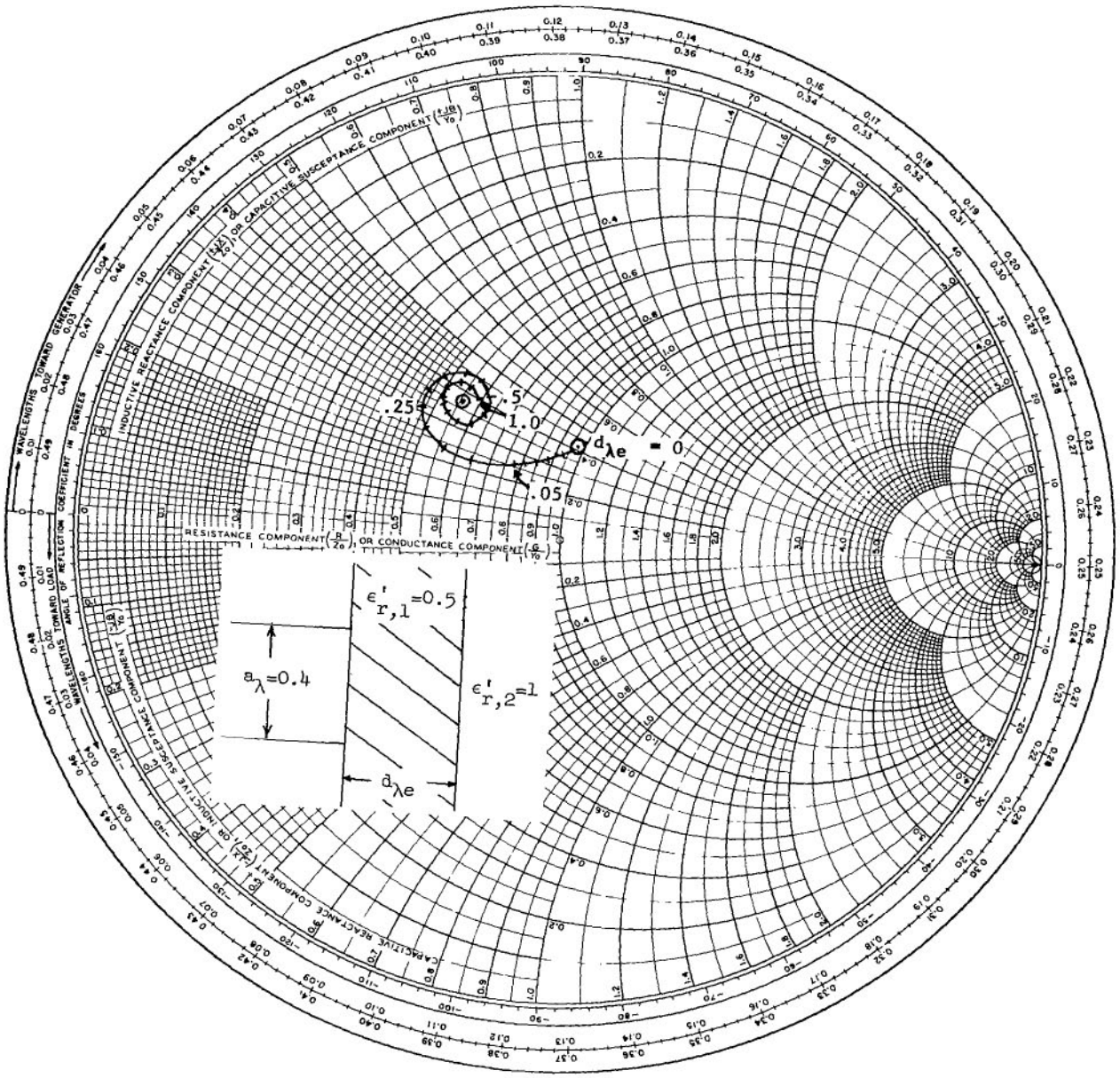

(a) $\varepsilon'_{r,1} = 0.5$. Continued.

Figure 6.- Continued.

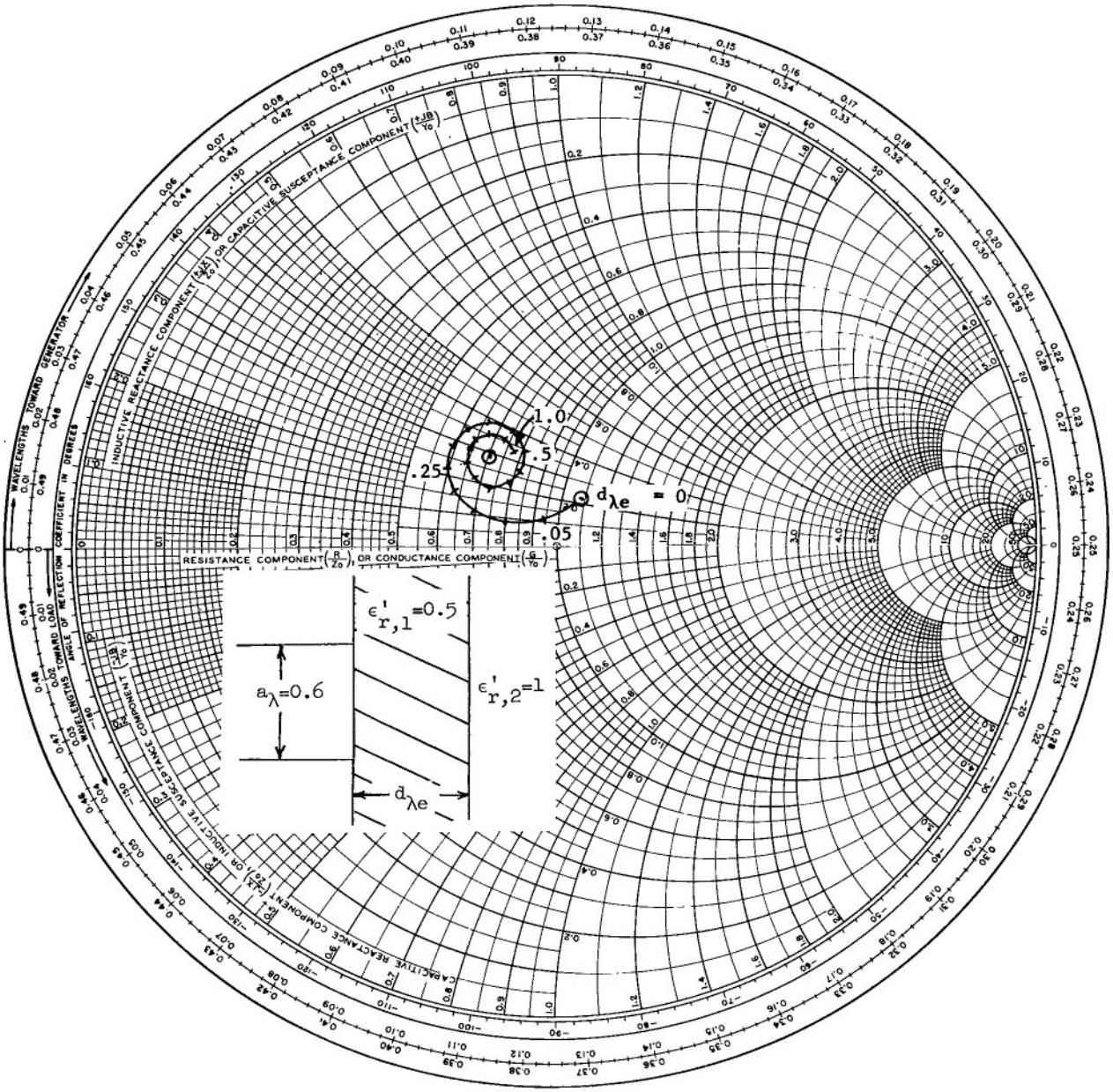

(a) $\epsilon'_{r,1} = 0.5$. Concluded.

Figure 6.- Continued.

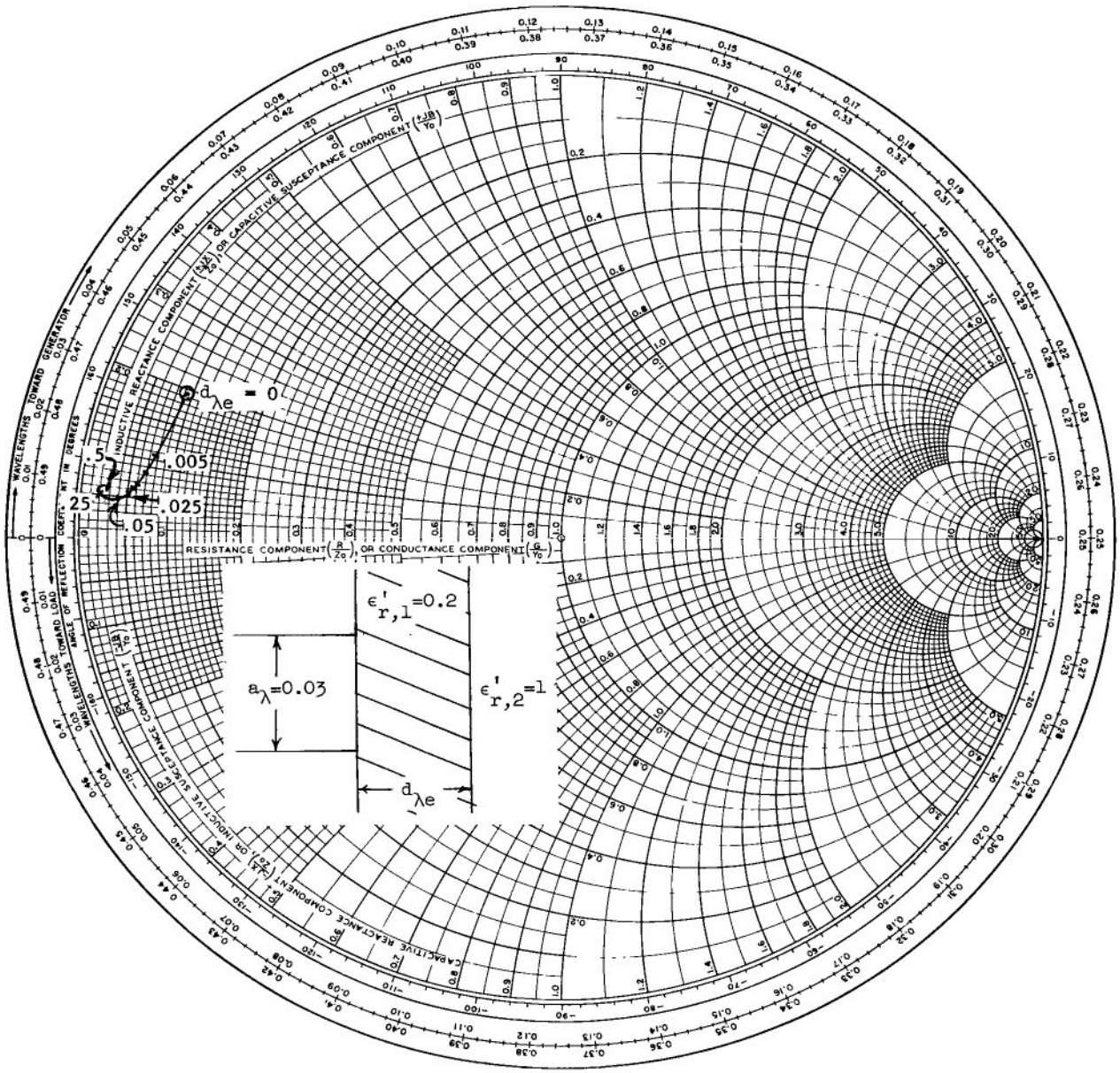

(b) $\epsilon'_{r,1} = 0.2$.

Figure 6.- Continued.

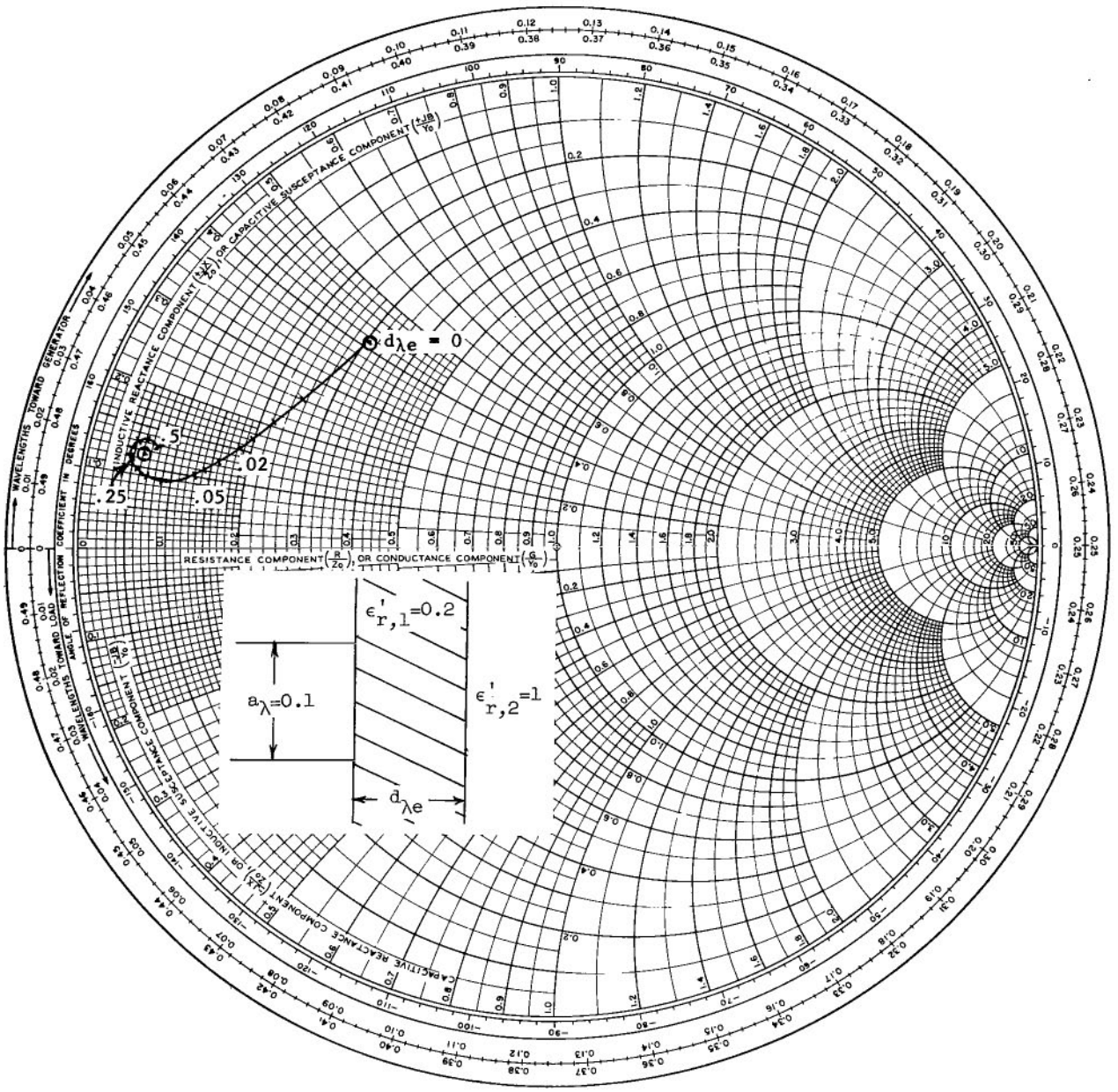

(b) $\epsilon'_{r,1} = 0.2$. Continued.

Figure 6.- Continued.

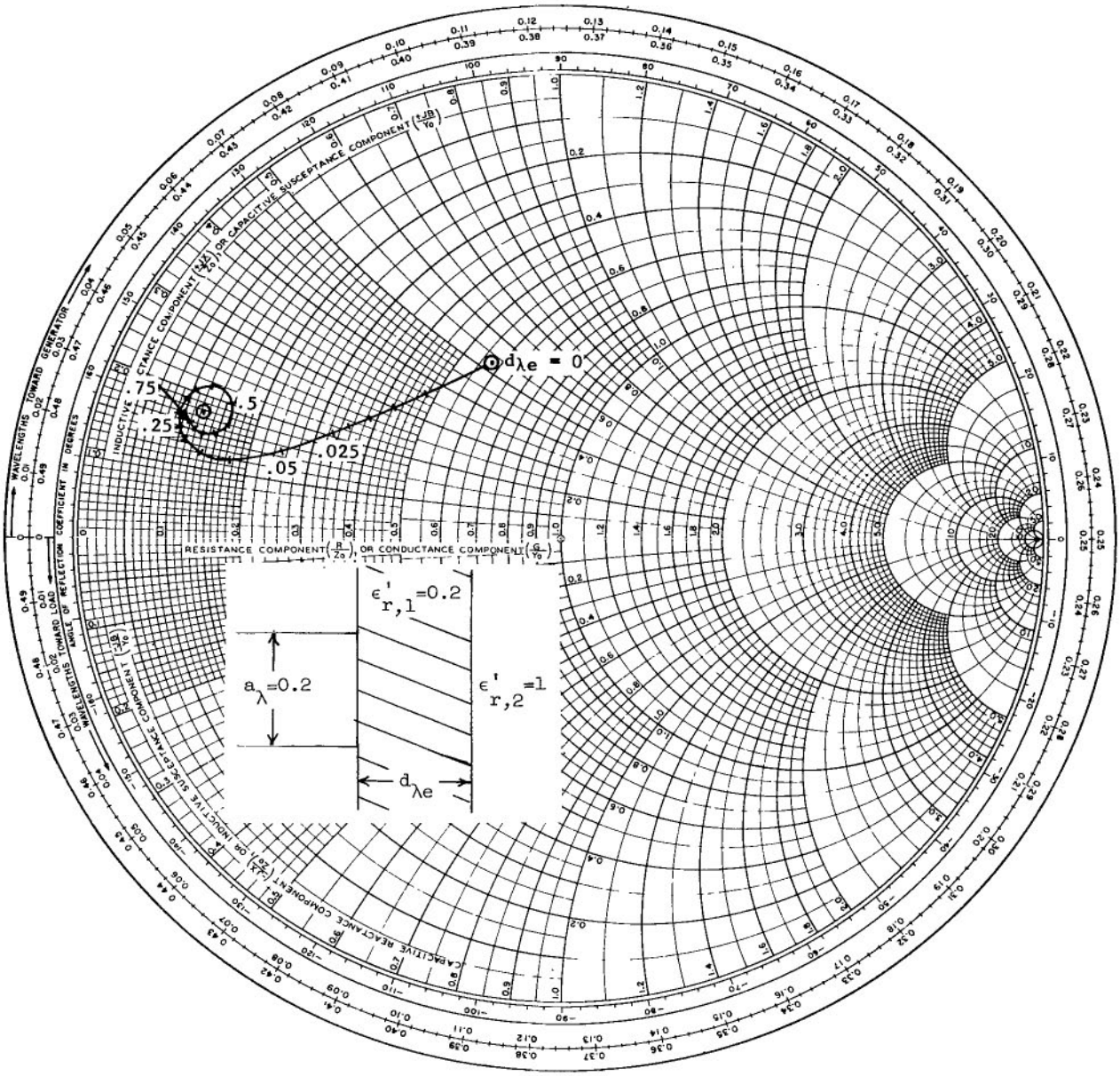

(b) $\epsilon'_{r,1} = 0.2$. Continued.

Figure 6.- Continued.

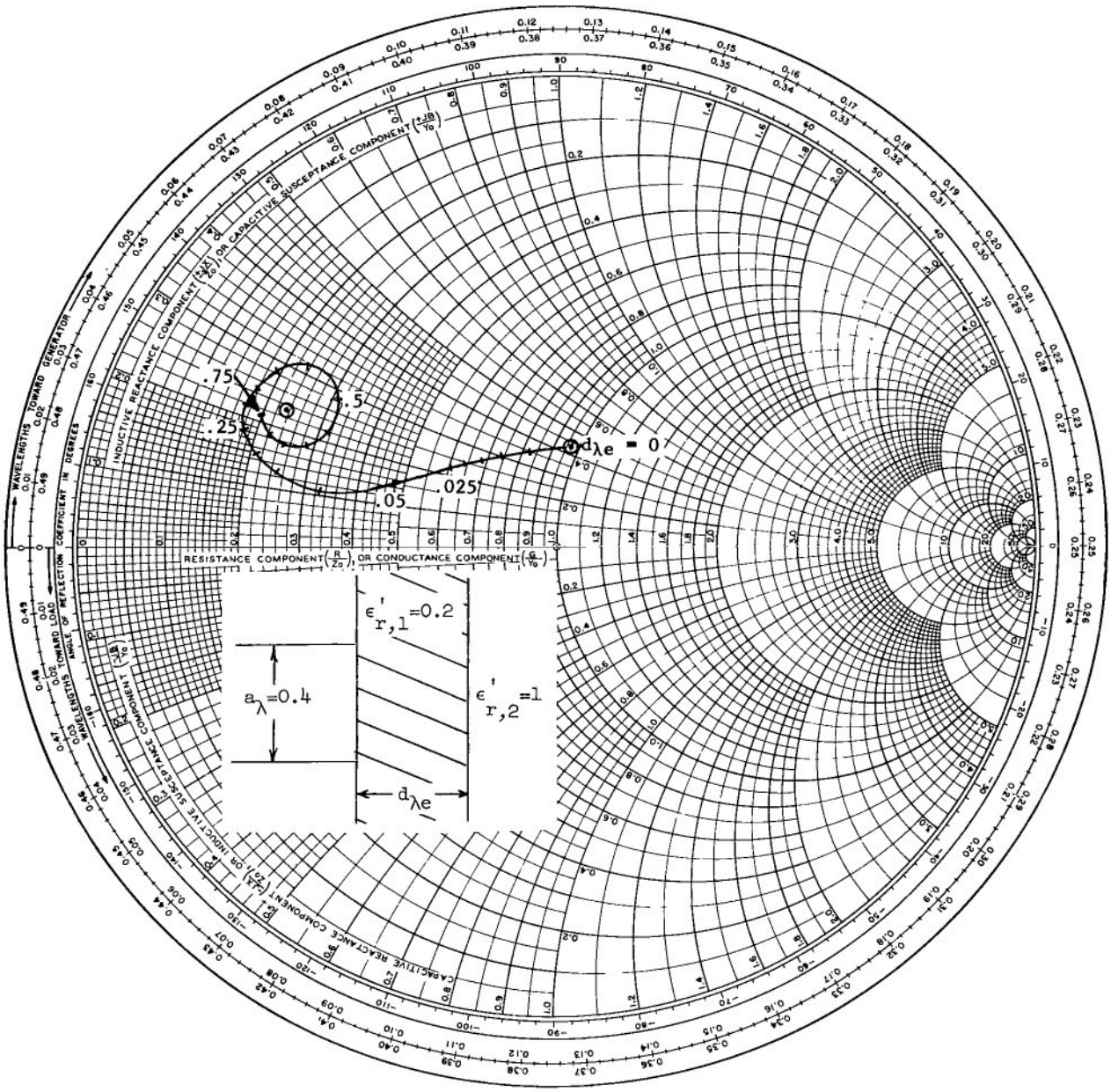

(b) $\epsilon'_{r,1} = 0.2$. Continued.

Figure 6.- Continued.

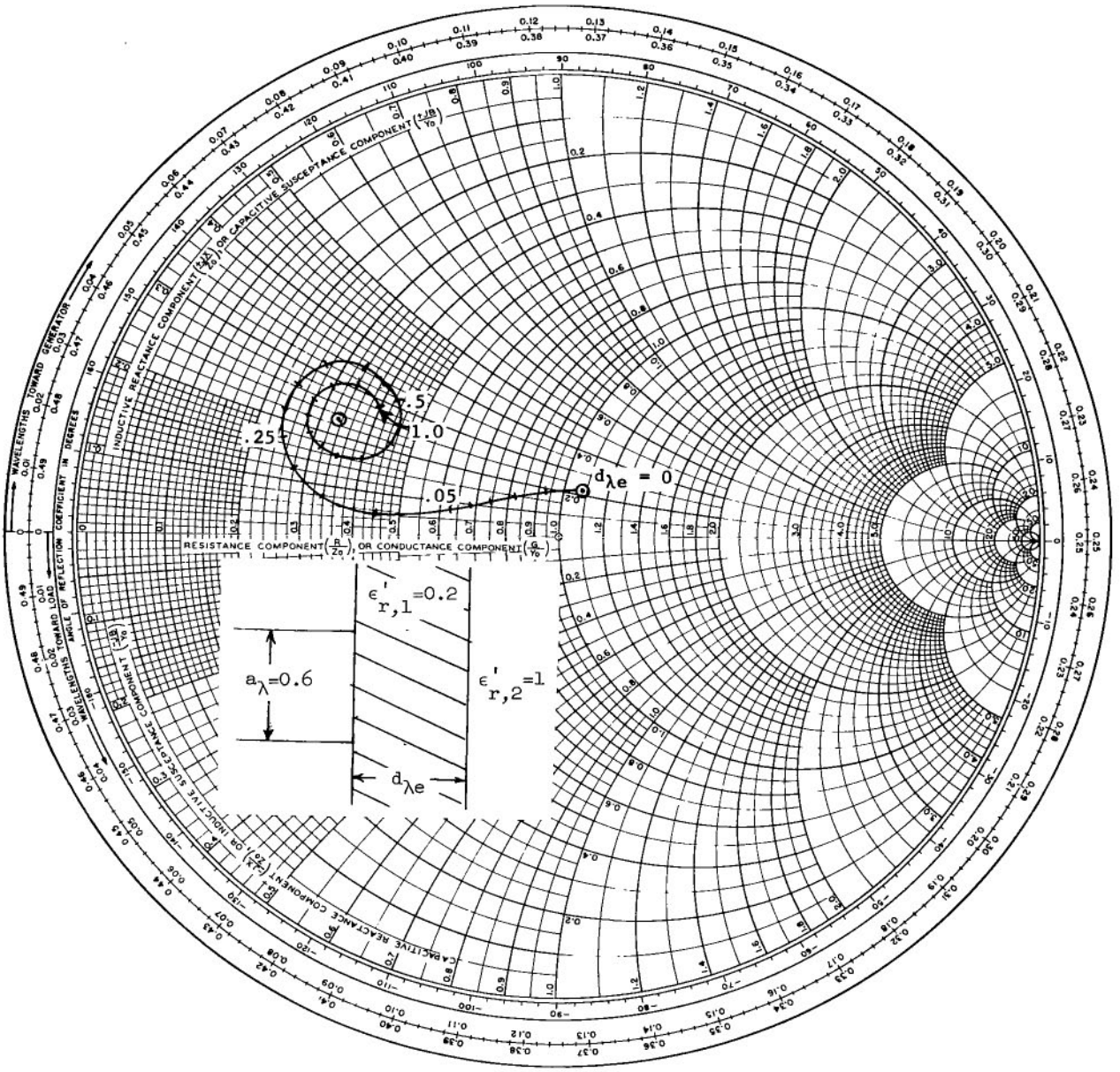

(b) $\epsilon'_{r,1} = 0.2$. Concluded.

Figure 6.- Continued.

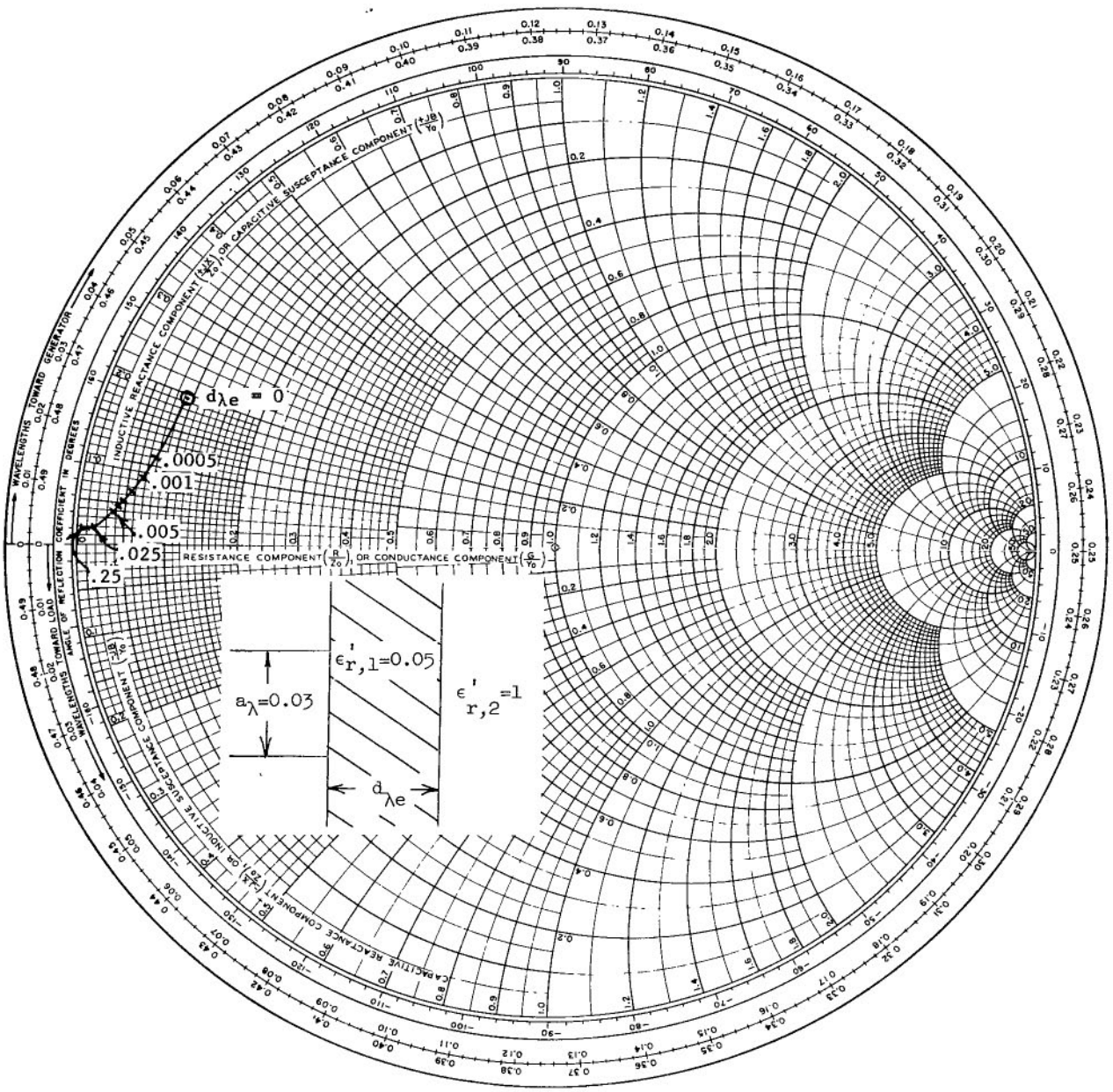

(c) $\epsilon'_{r,1} = 0.05$.

Figure 6.- Continued.

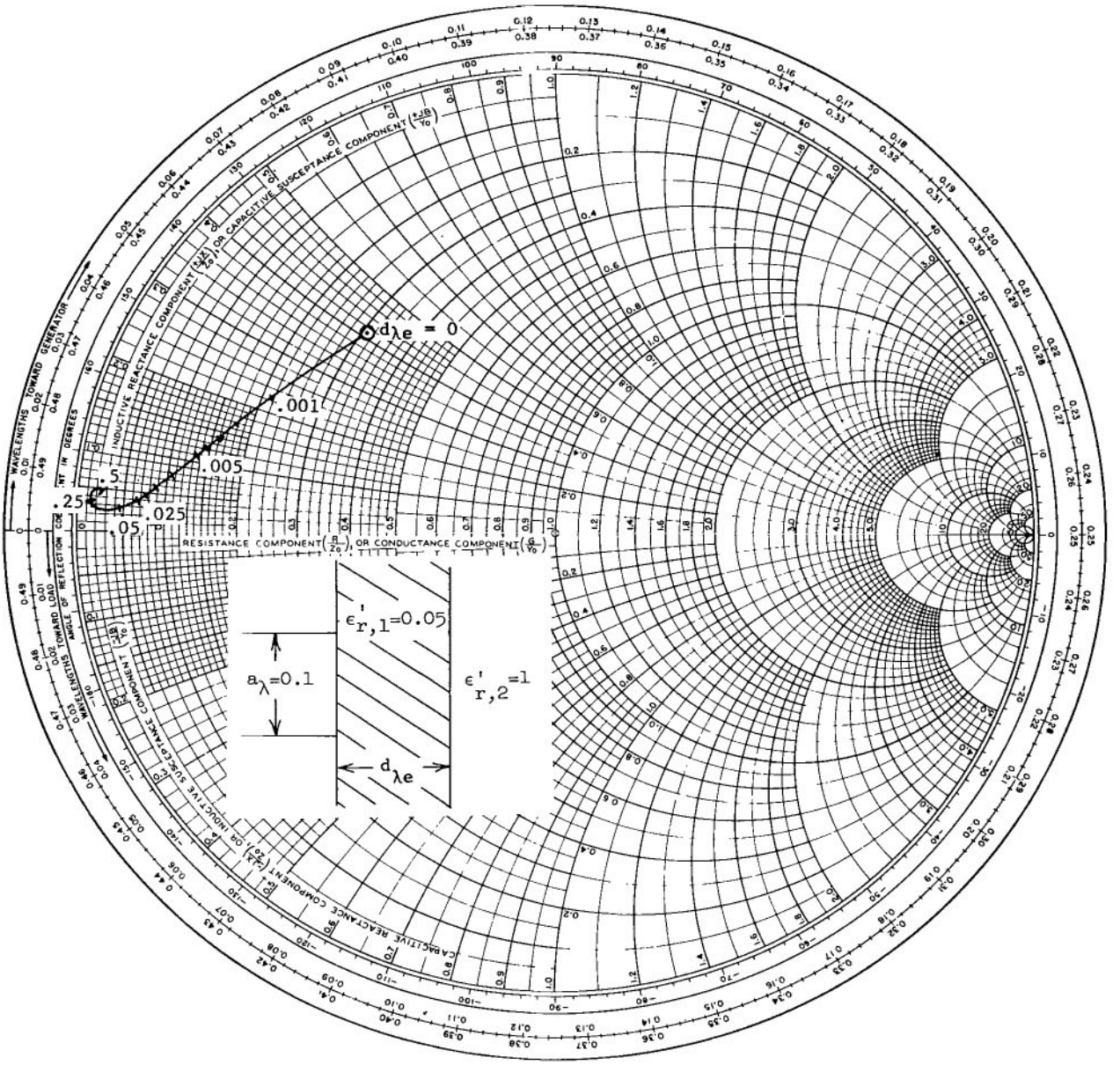

(c) $\epsilon'_{r,1} = 0.05$. Continued.

Figure 6.- Continued.

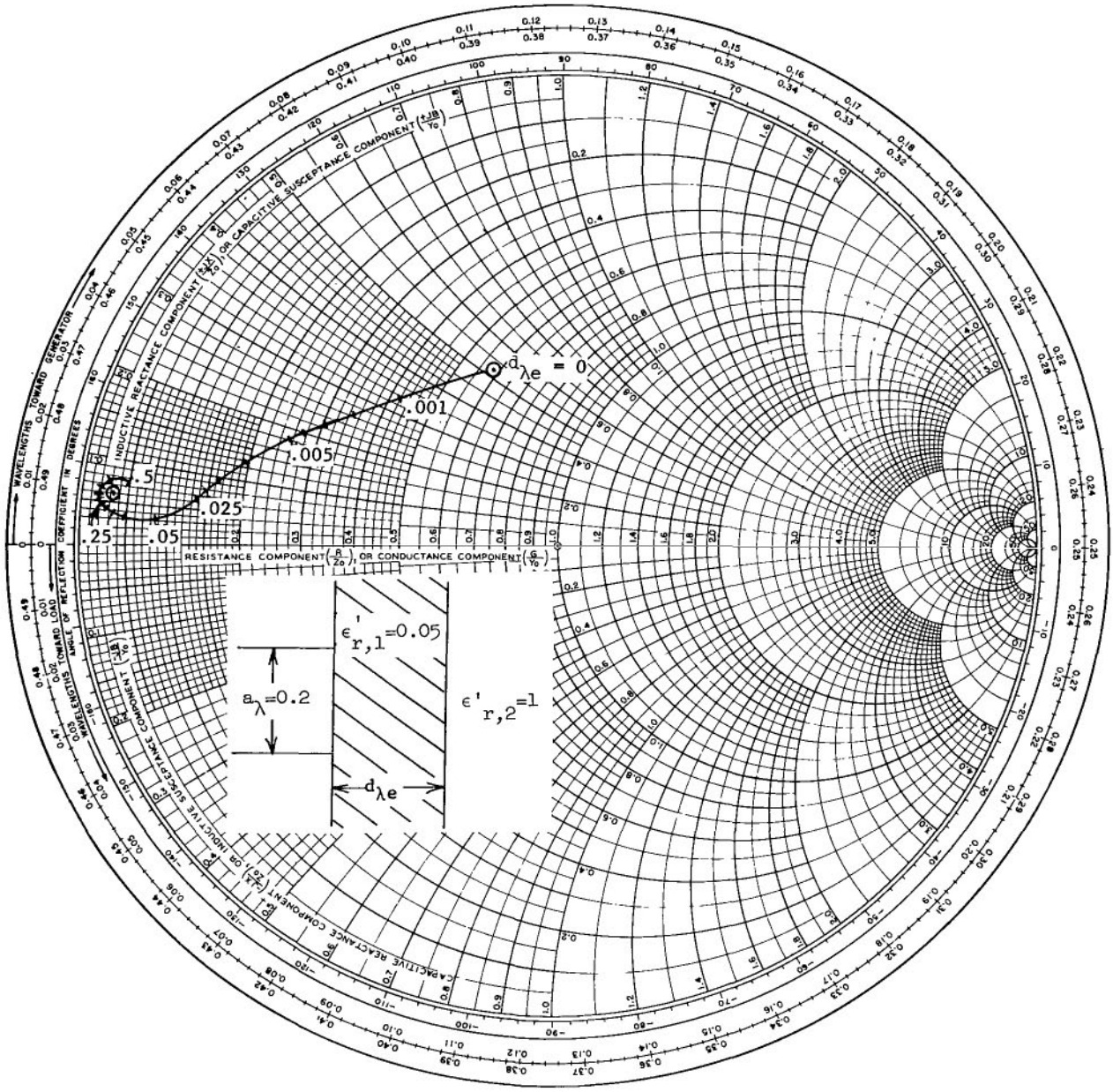

(c) $\epsilon'_{r,1} = 0.05$. Continued.

Figure 6.- Continued.

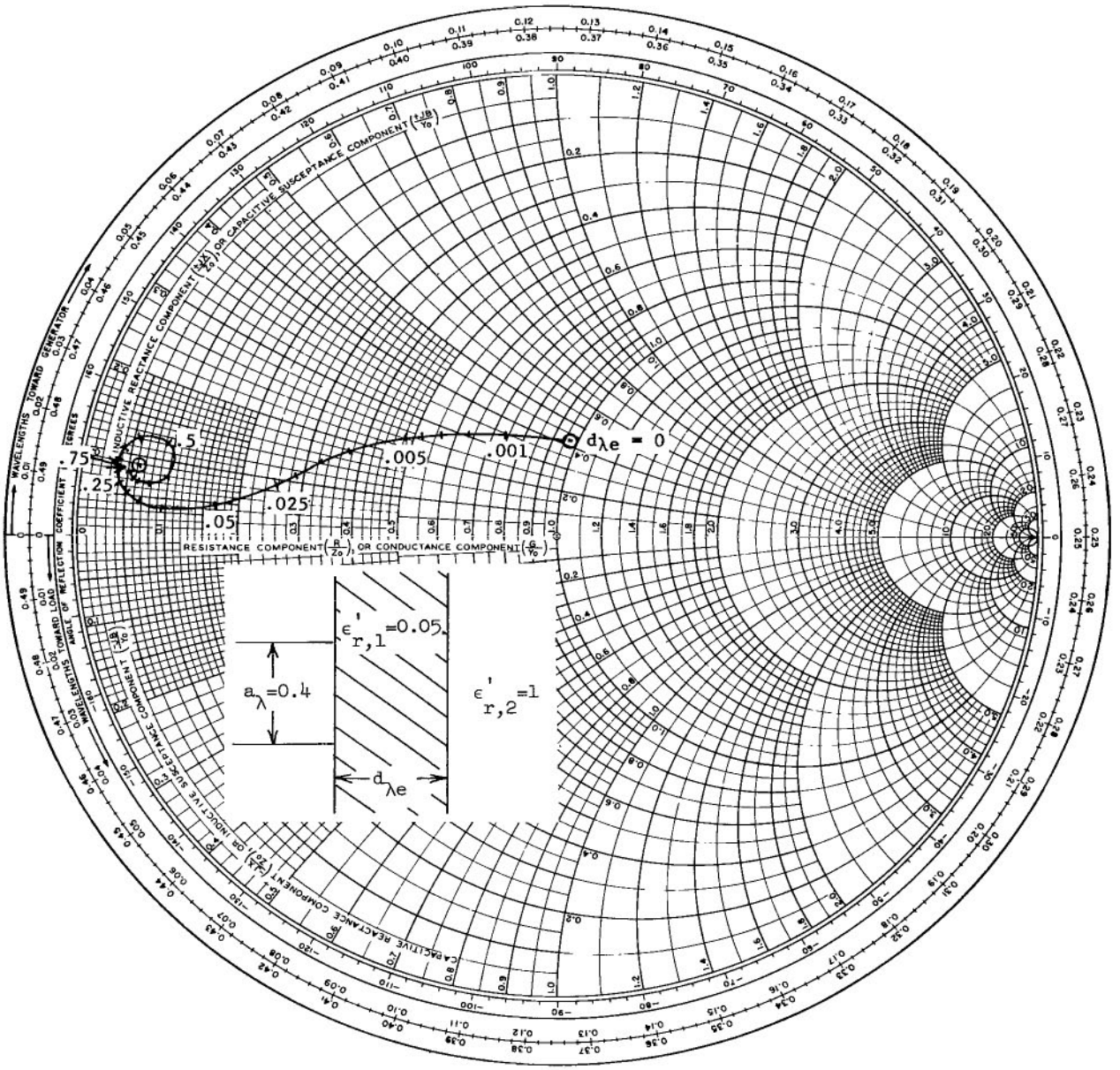

(c) $\epsilon'_{r,1} = 0.05$. Continued.

Figure 6.- Continued.

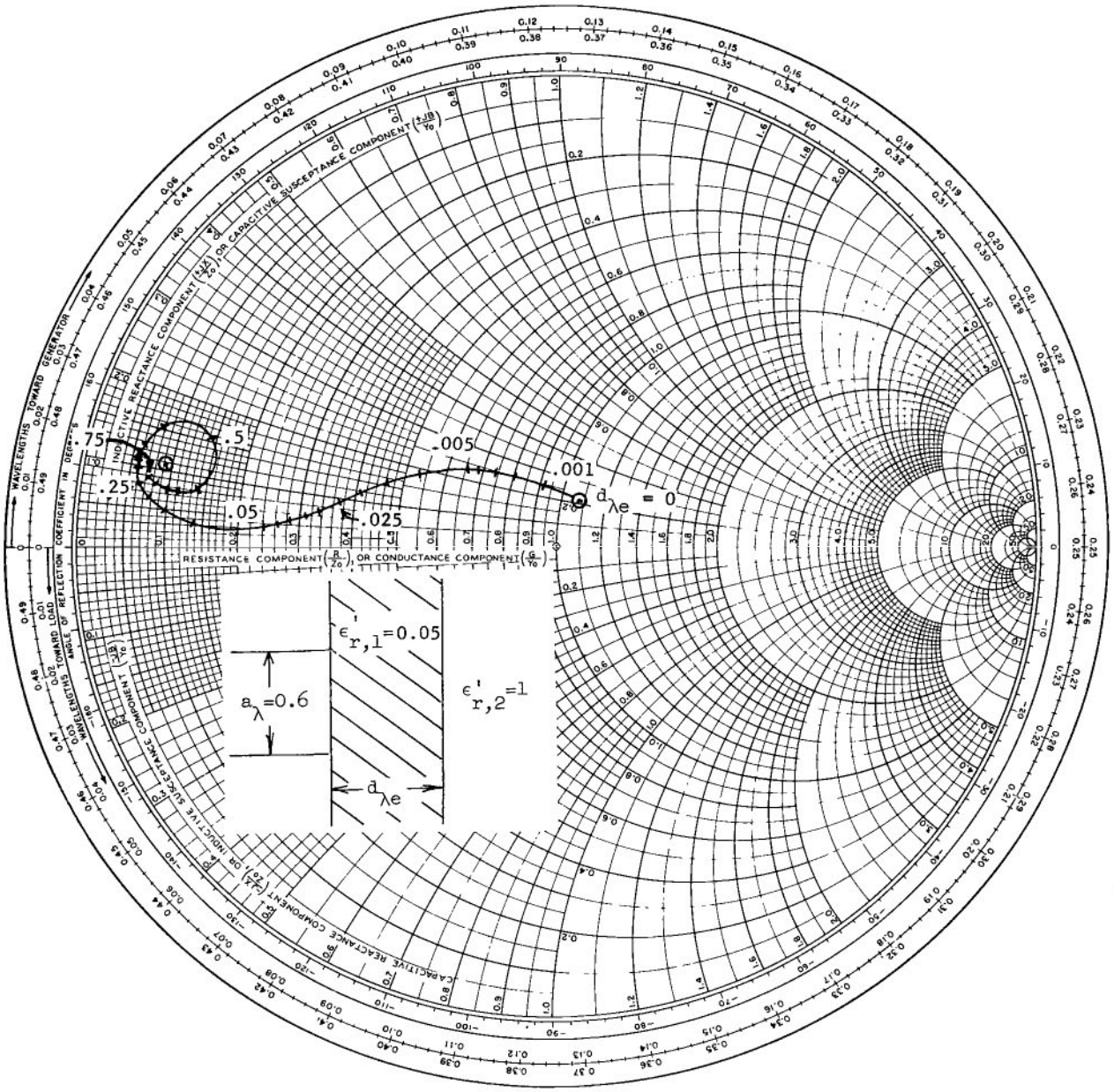

(c) $\epsilon'_{r,1} = 0.05$. Concluded.

Figure 6.- Concluded.

NATIONAL AERONAUTICS AND SPACE ADMINISTRATION
WASHINGTON, D. C. 20546

OFFICIAL BUSINESS

FIRST CLASS MAIL

POSTAGE AND FEES PAID
NATIONAL AERONAUTICS AND
SPACE ADMINISTRATION

"The aeronautical and space activities of the United States shall be conducted so as to contribute . . . to the expansion of human knowledge of phenomena in the atmosphere and space. The Administration shall provide for the widest practicable and appropriate dissemination of information concerning its activities and the results thereof."

—NATIONAL AERONAUTICS AND SPACE ACT OF 1958

NASA SCIENTIFIC AND TECHNICAL PUBLICATIONS

TECHNICAL REPORTS: Scientific and technical information considered important, complete, and a lasting contribution to existing knowledge.

TECHNICAL NOTES: Information less broad in scope but nevertheless of importance as a contribution to existing knowledge.

TECHNICAL MEMORANDUMS: Information receiving limited distribution because of preliminary data, security classification, or other reasons.

CONTRACTOR REPORTS: Scientific and technical information generated under a NASA contract or grant and considered an important contribution to existing knowledge.

TECHNICAL TRANSLATIONS: Information published in a foreign language considered to merit NASA distribution in English.

SPECIAL PUBLICATIONS: Information derived from or of value to NASA activities. Publications include conference proceedings, monographs, data compilations, handbooks, sourcebooks, and special bibliographies.

TECHNOLOGY UTILIZATION PUBLICATIONS: Information on technology used by NASA that may be of particular interest in commercial and other non-aerospace applications. Publications include Tech Briefs, Technology Utilization Reports and Notes, and Technology Surveys.

Details on the availability of these publications may be obtained from:

SCIENTIFIC AND TECHNICAL INFORMATION DIVISION

NATIONAL AERONAUTICS AND SPACE ADMINISTRATION

Washington, D.C. 20546